Master thesis

# Application of IR-based nanospectroscopic methods to study the interaction of Vancomycin with the bacterial cell wall of *Bacillus subtilis*


*Written by*

**Robin Schneider (78582)**

*Supervisors*

**Dr. Daniela Täuber**

**Prof. Dr. Torsten Stein**

Department Microscopy

Leibniz Institute for Photonic Technologies

# Contents

# Abbreviations

AFM: atomic force microscopy

BSA: bovine serum albumin

FTIR: Fourier transformation infrared spectroscopy

IR: infrared

IR s-SNOM: infrared scattering scanning near-field optical microscopy

kDa: kilo dalton

MCT: mercury cadmium telluride (-detector)

NAG: *N*-acetylglucosamine

NAM: *N*-acetylmuramic acid

NIR: near infrared

OD: optical density

O-PTIR: optical-photothermal infrared spectroscopy

PCA: principal component analysis

PiFM: photo-induced force microscopy

PTIR: photothermal-induced resonance microscopy

QCL: quantum cascade laser

RGB: red, green, blue

rpm: rounds per minute

TDA: topological data analysis

VIS: visible

## Abstract

Infrared (IR) vibrational spectroscopy is already known to be an ideal technique for biomedical cell analysis and in this way the IR-based nanospectroscopic methods, optical-photothermal IR spectroscopy (O-PTIR) and photo-induced force microscopy (PiFM), are likewise promising in this scientific field, since these methods are non-invasive, non-destructive, and sensitive, too. Additionally, O-PTIR and PiFM can overcome the diffraction limit of classical IR spectroscopy, either with a visible detection probe or with mechanical scanning with a sharp tip based on atomic force microscopy. Both approaches were used to study the interaction between the glycopeptide-antibiotic Vancomycin and the bacterial cell wall of the Gram-positive bacterium *Bacillus subtilis*. This work demonstrates the suitability of both new methods, O-PTIR and PiFM, for the detection of chemical differences in the form of specific vibrational bands between the with Vancomycin-treated bacteria and the untreated control. Furthermore, PiFM enables imaging the highly localized action of Vancomycin at division sites of single bacteria, due to its sub-10 nm spatial resolution.

# 1 Introduction

Infrared (IR) vibrational spectroscopy is known to be an ideal technique for biomedical cell analysis, since it is non-invasive, non-destructive and sensitive (Baker *et al.*, 2016). In this way it has been widely used for chemical identification and quantitative analysis, since it delivers information about specific functional groups and chemical characteristics of molecules through the direct coupling of IR-radiation to vibrational transitions (Le Wang *et al.*, 2019; Li *et al.*, 2020). However, IR spectroscopy is only able to measure an average signal of whole cells, instead of single reaction sites (Li *et al.*, 2020). The spatial resolution of IR microscopy and spectroscopy is diffraction limited (Le Wang *et al.*, 2019). The use of a visible probe to detect the photothermal IR-effect of the sample in optical-photothermal IR-spectroscopy (O-PTIR) can overcome this, on the long wavelengths of incident IR-radiation depending, diffraction limit (Olson *et al.*, 2020). The focal size of the visible laser, which is on the submicron scale determines the spatial resolution of O-PTIR and is independent of the used IR wavelengths (Baden *et al.*, 2020). A recent study demonstrates the ability of this novel far-field infrared imaging technique as a tool to monitor cellular uptake of stable isotope-labeled compounds by *Escherichia coli* at single-cell level (Lima *et al.*, 2021). It also could be shown that O-PTIR enables the analysis of subcellular structures in both, fixed and live cells under aqueous conditions and the study demonstrated, that the protein secondary structure and lipid-rich bodies can be identified on the submicron scale with O-PTIR (Spadea *et al.*, 2021). Atomic force microscopy (AFM)-based methods, such as infrared scattering scanning near-field optical microscopy (IR s-SNOM) or photothermal-induced resonance microscopy (PTIR) provide another way to overcome the optical diffraction limit. IR s-SNOM uses optical detection of the scattered light from a metallic AFM-tip and provides a spatial resolution of approximately 20 nm (Xiao & Schultz, 2018). Though s-SNOM spectra often do not correspond to the far-field IR-absorption spectra, what makes the chemical identification challenging and also the sensitivity for soft matter, such as biological samples, is limited (Le Wang *et al.*, 2019; Xiao & Schultz, 2018). The measuring of the samples thermal expansion, which is induced by IR absorption, in contact-mode AFM is called PTIR and offers also 20 nm spatial resolution (Katzenmeyer *et al.*, 2015). An even more surpassing spatial resolution below 10 nm can be realized with photo-induced force microscopy (PiFM), which measures the photo-induced force between the AFM-tip and the sample. Likewise, the tapping-mode operation of PiFM is superior to the contact-mode used in PTIR because tapping-mode avoids irreversible damage of the sample surface by scratching (Le Wang *et al.*, 2019). Thereby minimal tip-sample interaction makes PiFM ideal for soft biological samples (Nowak *et al.*, 2016). Already in 2008 a study demonstrated the ability of PTIR to perform nanochemical mapping of water-immersed cells with roughly 50 nm spatial resolution (Mayet *et al.*, 2008).

That PiFM with a sub-10 nm resolution is likewise well suited for biological samples was reported for proteinaceous collagen fibers, bovine serum albumin (BSA) proteinaceous monolayers and the visualization of individual protein cages by scanning the amide I and II bands (Cristie-David *et al.*, 2019; Li *et al.*, 2020; Wickramasinghe & Park, 2015). Moreover, PiFM enables label-free detection of single protein particles with molecular weights down to 30 kDa of biotoxins (Ji *et al.*, 2019). For bacterial peptidoglycan isolates from *Enterococcus faecium*, different contents of peptide in the sample could be revealed with a spatial resolution down to 8 nm with PiFM (Le Wang *et al.*, 2019).

## 1.1 The interaction of *Bacillus subtilis* and Vancomycin as model system

*Bacillus subtilis* is a Gram-positive bacterium and ubiquitous spread in soil and can also be found in the gastrointestinal tract of humans (Errington & van der Aart, 2020). These rod-shaped bacteria are typically flagellated several times (Müller, 2013). *Bacillus subtilis* can form endospores, allowing it to tolerate extreme environmental conditions (Madigan, 2005; Stein, 2020). Further, *bacillus subtilis* is the best studied Gram-positive bacterium and serves as model organism to study bacterial chromosome replication and cell differentiation (Errington & van der Aart, 2020; Stein, 2005). In comparison to Gram-negative bacteria, like *Escherichia coli*, whose cell wall only contains less than 10 nm peptidoglycan, Gram-positive bacteria have a thick peptidoglycan layer (20 - 80 nm) as main cell wall component (Madigan, 2005). This on peptidoglycan-based cell wall of *Bacillus subtilis* can be affected by the glycopeptide antibiotic Vancomycin (Gilbert *et al.*, 2007; Kahne *et al.*, 2005; Pereira *et al.*, 2007). Vancomycin is a Lipid II binder and interacts with the dipeptide D-Ala-D-Ala, the terminal group of the peptidoglycan precursor (Burkard & Stein, 2008; Molinari *et al.*, 1990). By blocking this essential substrate, Vancomycin inhibits the cross-linkage for bacterial cell wall formation (Aktories *et al.*, 2017; McComas *et al.*, 2003). The interaction is based on five hydrogen bonds (Fig. 1) between D-Ala-D-Ala and the flexible side chains of Vancomycin (Rao *et al.*, 1997). The flexible side chain residues consisting of an asparagine and a N-methyl-leucin becomes stiff during the interaction, even if they are not directly involved in the H-bond formation (Wang *et al.*, 2018). Additionally, the electrostatic interaction between the N-terminal amine of Vancomycin and the carboxylate of the D-Ala-D-Ala play an important role in the binding (Rao *et al.*, 1997).

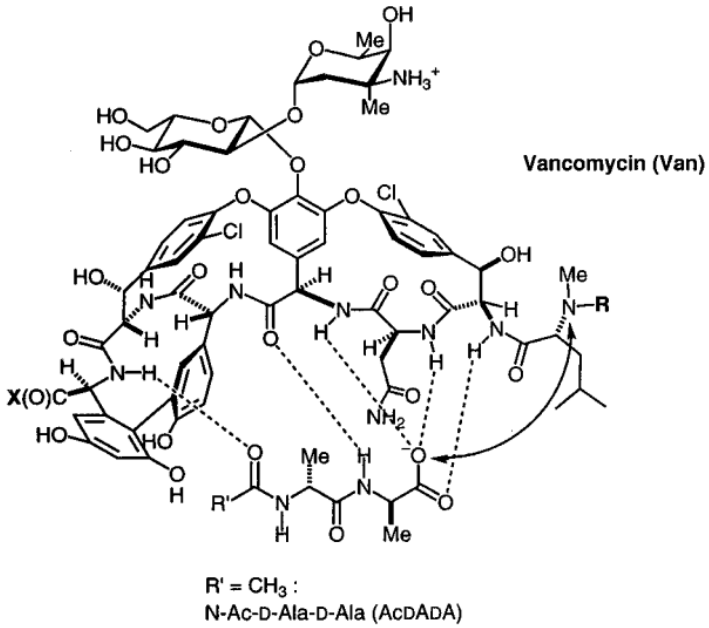


*Figure 1: The interaction of Vancomycin with the D-Ala-D-Ala terminal group of the peptidoglycan precursor is based on five hydrogen bonds (Rao et al., 1997)*

In general peptidoglycan or murein is a polymer consisting of a sugar and an amino acid component (Wheeler *et al.*, 2011). The sugar component consists of alternating residues of β-(1,4) linked *N*-acetylglucosamine (NAG) and *N*-acetylmuramic acid (NAM) (Hayhurst *et al.*, 2008; Vollmer & Bertsche, 2008). A peptide chain of three to five amino acids is attached to the NAM (Tortora *et al.*, 2007). The binding of Vancomycin to the terminal D-Ala-D-Ala dipeptide of this peptide chain prevents cross-linking of the subunits NAM and NAG that form the backbone strands of the peptidoglycan and are essential to a functioning bacterial cell wall (Li *et al.*, 2018; McStrother, 2011). If Vancomycin has bound to the peptide chain, the cell wall cross-linking enzyme (DD-transpeptidase) cannot bind, and cell wall formation is disturbed (Fig. 2). However, in resistant bacteria, the last D-Ala residue can be replaced by a D-lactate, consequently Vancomycin is ineffective and cross links can form (McStrother, 2011; Stogios & Savchenko, 2020; Tortora *et al.*, 2007).

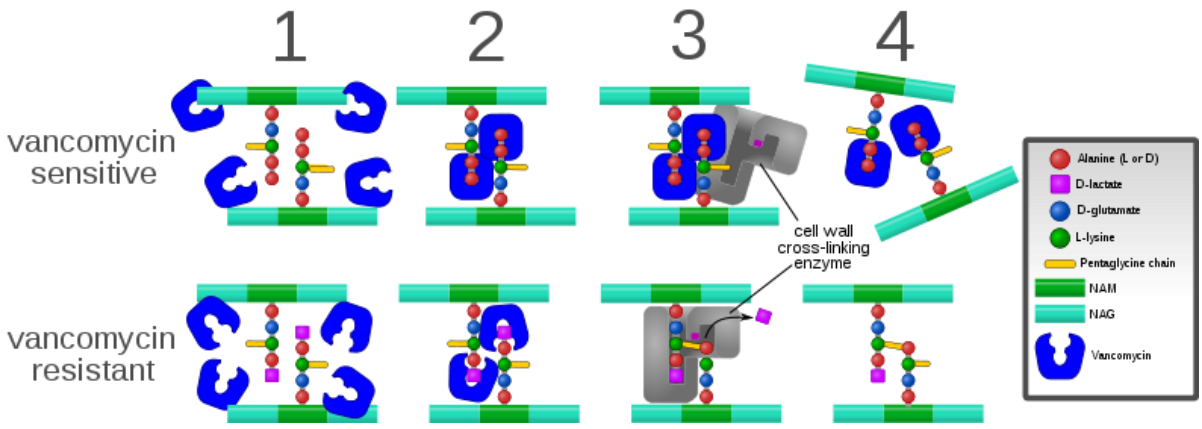


*Figure 2: Vancomycin mechanism of action and one exemplary way of resistance (McStrother, 2011)*

## 1.2 Objectives

This work demonstrates the possibilities and current limitations of IR-based nanospectroscopic methods to study biomedical interactions between biomacromolecules like antibiotics with single cells. In this case, exemplary, the interaction between the glycopeptide-antibiotic Vancomycin with the bacterial cell wall of *Bacillus subtilis* is analyzed with two nanospectroscopic methods, optical-photothermal IR spectroscopy and photo-induced force microscopy. For comparison Fourier transformation infrared spectroscopy is used.

# 2 Theoretical aspects of IR-based vibrational spectroscopy

IR -absorption occurs when the energy of incident IR-light with general wavelengths between 800 nm and 1 mm (E = hν) matches the energy difference ΔE between two vibrational states of a molecule (Baker *et al.*, 2016). These energy differences ΔE are chemically characteristic for each covalent chemical bond in a molecule, such that every IR-active molecule provides a characteristic IR-absorption spectrum. But in general, only molecules with a changeable or inducible dipole moment are IR-active. Further, the excitation by IR-light induces various phenomena in the samples, like thermal expansion or a change in the molecular electromagnetic dipole, which can be exploited by different techniques.

## 2.1 Fourier Transformation IR spectroscopy (FTIR)

The most established form of infrared spectroscopy is the Fourier transformation infrared spectroscopy (FTIR). The Fourier transformation is used for enhancement of the signal-to-noise ratio because typically IR-absorption spectra are weak. For signal detection often liquid nitrogen cooled mercury cadmium telluride (MCT) detectors are used in so called "photoconductive mode". There photons from incident light promote electrons from the valence band to the conduction band, so that an increase in conductivity is a measure of the photon flux (Salzer & Siesler Heinz W., 2014). The spectral range is limited due to the fact, that these detectors do not respond to radiation below 750 wavenumbers. The spatial resolution of FTIR is mainly diffraction limited by the radius of the longest wavelength of the incident IR-light (for mid-IR: 2,5 - 25 µm). Further the refractive index of the used medium (for air: n = 1.0) limits the spatial resolution (Salzer & Siesler Heinz W., 2014).

## 2.2 Optical-photothermal infrared spectroscopy (O-PTIR)

The optical-photothermal IR spectroscopy (O-PTIR) uses a visible (VIS) or near-IR (NIR) probe to detect the photothermal IR-effect. O-PTIR operates with high speed, pulsed and tunable IR lasers, which are focused onto the sample surface (Fig. 3). If the incident IR laser is tuned to a wavelength, that induces IR absorption, the excited regions of the sample rapidly heat up and the photothermal response is measured via a visible laser beam, focused to a much smaller spot than the IR beam (Photothermal Spectroscopy Corporation, 2020). Thereby O-PTIR provides a better lateral resolution than FTIR due to the VIS or NIR beam wavelength of the detection laser and in this way IR spectroscopy and chemical imaging are independent of the IR wavelength. Such that it is possible to get lateral resolutions between 0,5 and 1 µm. The measured photothermal signal is proportional to the thermal expansion of the sample, the absorbed energy per unit area $U_{abs}$ and the duration of the excitation. Additionally, the thermal expansion is proportional to the thickness of the sample (Baker *et al.*, 2016).

Moreover, even if O-PTIR measures in reflection mode the absorption spectra show FTIR transmission-like quality (Photothermal Spectroscopy Corporation, 2020).

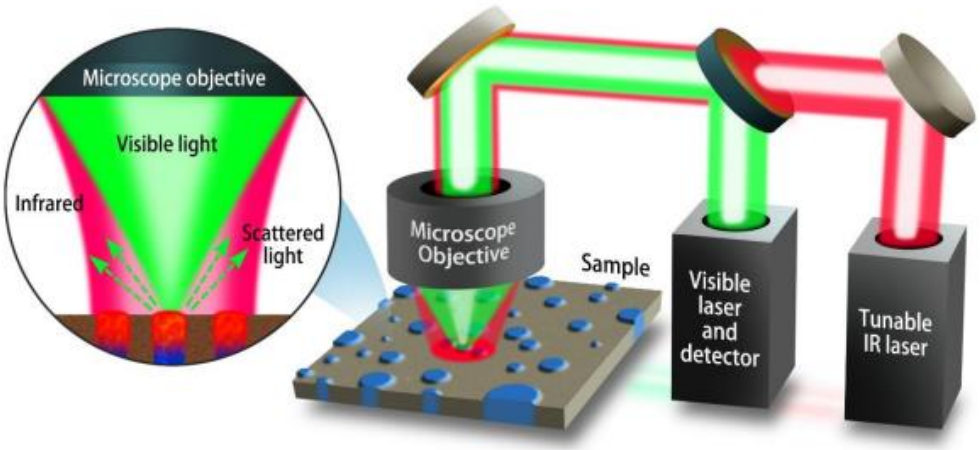


*Figure 3: O-PTIR setup (Photothermal Spectroscopy Corporation, 2020)*

## 2.3 Photo-induced force microscopy (PiFM)

Photo-induced force microscopy (PiFM) is based on atomic force microscopy (AFM), in which the sample surface is mechanically scanned with a sharp tip and atomic forces between the tip and the sample bend the cantilever, on which the tip is mounted. The interaction force $F_{ts}$ between tip and sample depends on the tip-sample distance z and the spring constant of the cantilever. Examples for these acting forces are Van der Waals-, capillary-, electrostatic- or magnetic dipole-forces and chemical bonding. For signal detection the bending of the cantilever is measured, whereby conclusions to the acting force between sample and tip can be drawn. There are two different general operation modes in AFM. On the one hand, in the constant force contact mode the interaction force $F_{ts}$ is kept constant and on the other hand there is a driven oscillation near the resonance frequency of the cantilever which is controlled via feedback in the dynamic mode. Further, the dynamic mode can be differentiated into non-contact mode and intermitting (tapping) mode (Lottspeich & Engels, 2012).

For PiFM comes in addition that the sample molecules are excited with IR-light. To this aim, mostly mid-IR (MIR) light is used. MIR light interacts with sample molecules in various ways. On the one hand it induces a change in electromagnetic dipole $\mu_s$ and on the other hand it induces, on-thermal-expansion-based, interaction forces (e.g., effective Van der Waals forces), but the exact composition of this interaction force is still a current research subject (Jahng *et al.*, 2016; Jahng *et al.*, 2018). PiFM also uses mechanical detection of the interaction force, which is mostly measured in an attractive regime, between the sample and a metallic AFM-tip. In general, this in z-direction acting force is in a range of a few pN, what enables a high lateral resolution below 10 nm (Li *et al.*, 2020).

For so called heterodyne detection in dynamic AFM-mode the cantilever is driven at its second mechanical resonance $f_1$ (first order eigenmode) and the detection of the PiFM signal is carried out at the first mechanical resonance $f_0$ (zeroth order eigenmode). Further the incident light of tunable quantum cascade lasers (Fig. 4) is polarized along the tip axis and pulsed at the frequency $f_m = f_1 - f_0$ for signal amplification (Le Wang *et al.*, 2019).

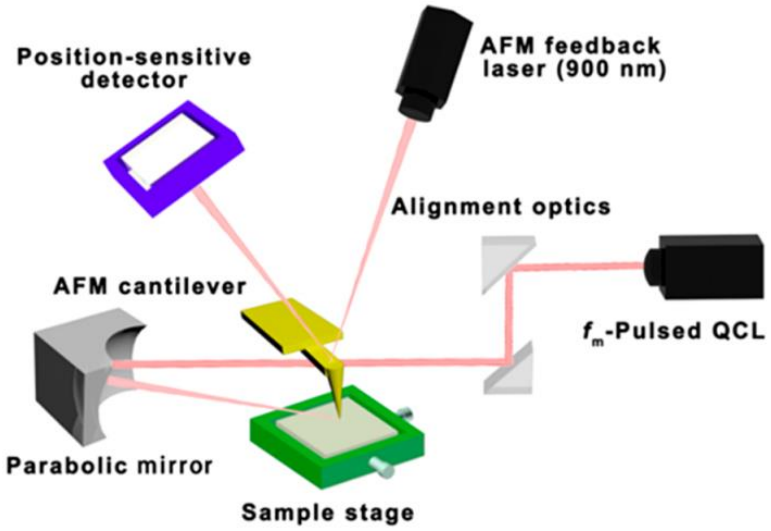


*Figure 4: PiFM setup (Li et al., 2020)*

## 2.4 Imaging and mapping

Spectroscopic imaging is like taking a photo in which the intensity is measured simultaneously from the whole region of interest with one wavelength or a narrow part of the spectrum (Badger, 2017). In contrast a whole spectrum or just one wavelengths is acquired, for each pixel or line, sequentially in spectroscopic mapping (Baker *et al.*, 2016). For so called "hyperspectral imaging" an image of the sample is recorded simultaneously with more than 10 wavelength regions (Salzer & Siesler Heinz W., 2014). PiFM is all about mechanical, sequential scanning of the sample surface, thus according to the spectroscopic definition, it is about mapping. But in AFM surroundings this is called scanning (Lottspeich & Engels, 2012). Hence, in this work for PiFM in case of single wavenumber acquisition the result is called "scan" and if one or more wavenumber regions are recorded, "hyperspectral scan" is used.

# 3 Material and methods

## 3.1 Samples and sample preparation

A few µg D-Ala-D-Ala (SIGMA-ALDRICH) and Vancomycin hydrochloride hydrate (SIGMA-ALDRICH) in the form of powders were first solved in one milliliter water. For the interaction analysis 500 µl of each, D-Ala-D-Ala and Vancomycin, solution were mixed and left for 30 minutes reaction time. Afterwards a small amount of the sample solutions was dripped onto fresh $CaF_2$ substrates, air dried at room temperature and stored at 4-8 °C in the fridge before the measurements. *Bacillus subtilis* subsp. *spizizenii* (ATCC® 6633™) samples were cultivated in CASO broth (ROTH GmbH) overnight at 37 °C while shaking at 90 rpm. The overnight culture was used to inoculate a starter culture (60 ml) with an optical density (OD) of 1:10 at λ = 600 nm (Assmann *et al.*, 2015). Afterwards, the sample was divided into two 30 ml flasks, shaken for one hour at 30 °C and 10 µg/ml vancomycin were added to one of the flasks. After 15, 30 and 60 minutes a sample of treated and untreated *B. subtilis* was collected of each flask. Further, the six resulting bacteria samples were pelleted at 13000 g, washed twice in water, resuspended in 250 µl of water and 5 µl of each sample was dripped onto fresh or with Tergazyme® rinsed $CaF_2$ slides and air dried for 30 min at 50 °C. In the fridge at 4-8 °C the bacteria samples could be stored up to approximately two weeks.

## 3.2 FTIR measurements

The FTIR measurements were done using a VARIAN 620-IR FT-IR Imaging Microscope with a liquid nitrogen cooled mercury cadmium telluride (MCT) detector at 80 K with a resolution of 2 $cm^{-1}$, a spectral range of 750 to 4000 $cm^{-1}$ and the angle of incidence of IR-light is 0°. 8 scans for each sample absorption spectrum were acquired with an aperture of 100 x 100 µm for the D-Ala-D-Ala and Vancomycin samples. For the bacteria samples 32 scans for each sample absorption spectrum and maximum aperture was used to first collect a sample image in transmission mode. Continuing with averaging spectra from regions with either accumulated or single bacteria.

## 3.3 O-PTIR measurements

For O-PTIR measurements a mIRage™ system from Photothermal Spectroscopy Corporation (Santa Barbara, CA) integrated with a four-module pulsed quantum cascade laser (QCL) system, with a tunable range of 790 to 1806 $cm^{-1}$, a resolution of 2 $cm^{-1}$ and 10 scans for each sample spectrum, was used. Before the acquisition of spectra, an image at 1660 or 1655 $cm^{-1}$ was acquired and regions with either accumulated or single bacteria were selected. From there single spectra were measured.

For D-Ala-D-Ala and Vancomycin the edge of the drop was used for single spectra acquisition. The NIR detection laser was set at 785 nm and the angle of incidence of NIR and MIR-light is 0°. The IR laser power was modulated for each sample due to instrument performance and heat resistance of the sample between 21 and 47% of the maximum power. The probe power was set to 37%. All samples were measured in reflection mode on a reflecting metal coated substrate.

## 3.4 PiFM measurements

A VistaScope from Molecular Vista integrated with a four-module pulsed quantum cascade laser (QCL) system, with a tunable range of 770 to 1890 $cm^{-1}$ and a resolution of one wavenumber, was used. As already mentioned, the signal detection is done in dynamic mode, the, so called heterodyne detection (side band mode), with NCH-Pt 300 kHz noncontact cantilevers (type PPP-NCHPtx64-MB-10) from Nanosensors. Consequently, the cantilever was driven at its second harmonic resonance ($f_1 \approx 1750$ kHz), and the photo-induced force was detected at the first harmonic resonance ($f_0 \approx 280$ kHz). The pulses of the four tunable quantum cascade lasers (QCLs) were modulated at the difference $f_m = f_1 - f_0$ with 40 ns pulse duration. The angle of incidence of IR-light is 80° and the light of the four QCLs is co-aligned and linearly polarized in the plane of incidence (p-polarization). Spectra were acquired over 100 s with IR-light intensity clipped at 1-5% of the maximum intensity previously recorded in the power spectrum (see attachment Fig. A 1), depending on instrument performance. Scans of single wavenumbers were recorded with 5-30% IR-intensity and hyperspectral data with 5% of the maximum IR-laser power.

## 3.5 Data evaluation

Data pre-processing, spectra selection and RGB-overlay of single wavelengths chemical maps (O-PTIR) and scans (PiFM) were done with PTIRStudio v.4.3 for O-PTIR and SurfaceWorks 2.4 Release 22 and 23 for PiFM measurements. Background correction for FTIR spectra (BaselinePolyFit) and principal component analysis (PCA) for single spectra (MonIRana) and hyperspectral scans (HyPIRana) were carried out with in-house python programs provided by Mohammad Soltaninezhad and Sebastian Unger. All spectra were averaged, scaled, offset corrected, smoothed (Savitzky-Golay), min-max normalized, derived, subtracted, and displayed with SciDAVis 1.22. Vector normalization was done with Microsoft Excel 2016.

# 4 Results and discussion

## 4.1 D-Ala-D-Ala – Vancomycin interaction

To study the interaction of Vancomycin with the bacterial cell wall, first the single end group of the peptidoglycan precursor (NAM), the dipeptide D-Ala-D-Ala, was used with the aim of getting less background vibrations, which are not involved in the interaction. The method comparison of FTIR, O-PTIR and PiFM with the dried mixture of D-Ala-D-Ala and Vancomycin after 30 minutes reaction time in solution provides a good overview about the performances within the scope of the spectral resolution. Due to the lower wavenumber resolution (1 $cm^{-1}$) compared to O-PTIR and FTIR (2 $cm^{-1}$) and the higher lateral resolution, PiFM likewise shows a higher spectral resolution than the other methods. This and that the spectral resolution of O-PTIR is superior to FTIR, because of the better lateral resolution, is clearly visible at the amide I and amide II region around 1600 $cm^{-1}$, in which FTIR has only one peak, while O-PTIR has two separated vibrational bands (N-H amide I and C-N amide II) and PiFM provides sharper peaks and even a fine structure inside both separated bands (Fig. 5). Further, the most prominent vibrational bands of bio(macro)molecules are well separated for the analyzed mixture. There is the amide I band with C=O esters and N-H amine vibrations in the range of 1700 to 1600 wavenumbers and the amide II band with C-N and N-H vibrations (1600 – 1500 $cm^{-1}$). Between 1350 and 1200 $cm^{-1}$ there are the C-O carboxyl vibrations of the amide III band and between 1475 and 1375 $cm^{-1}$ there are the C-H methyl group bending's. C-O sugar and alcohol stretching's are to be found in the spectral region of 1200 to 1100 $cm^{-1}$. Other low intensity peaks at lower wavenumbers probably belong to C-H bending vibrations.

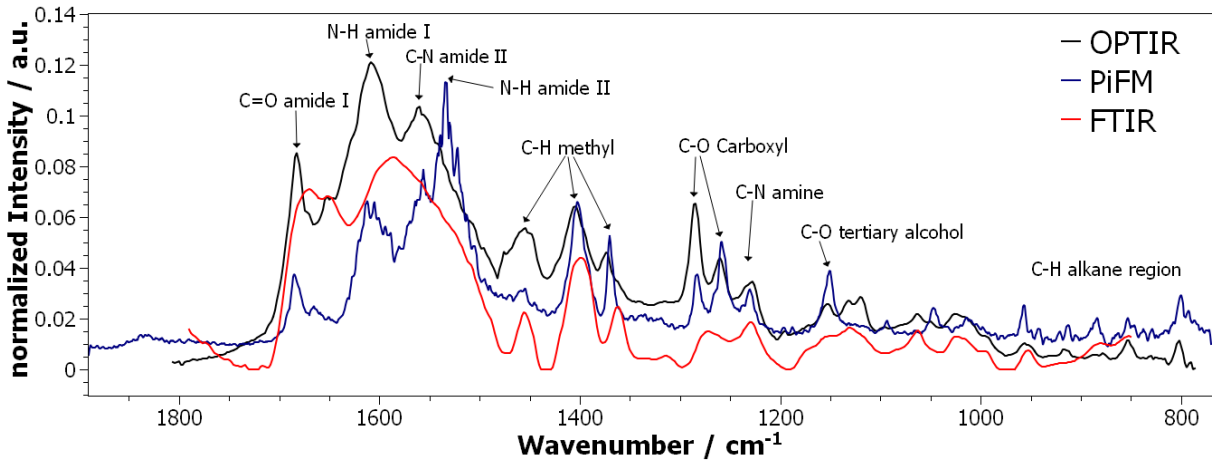


*Figure 5: Method comparison of FTIR, O-PTIR and PiFM with the D-Ala-D-Ala - Vancomycin mixture after 30 minutes reaction time*

The interaction analysis of the D-Ala-D-Ala and Vancomycin mixture after 30 minutes reaction time in comparison to pure D-Ala-D-Ala and pure Vancomycin with PiFM shows potential interesting spectral regions for the interaction, which have the biggest differences to the pure substances (Fig. 6). These are the N-H amine vibrations at 1612 $cm^{-1}$, 1534 $cm^{-1}$ and 1520 $cm^{-1}$ and the C-O carboxyl vibrations at 1283 $cm^{-1}$ and 1258 $cm^{-1}$. Additionally, some C=O ester vibrations between 1680 $cm^{-1}$ and 1640 $cm^{-1}$ and the C-O primary alcohol vibration at 1060 $cm^{-1}$ seem to be only present in pure Vancomycin. All these vibrations are potentially related to the hydrogen bonds, which are involved in the complex formation of D-Ala-D-Ala and Vancomycin (see Fig. 1). An exact assignment of each vibration to each hydrogen bond is impossible, since all amide vibrations show summarized bands of various vibrations of the same type close to each other.

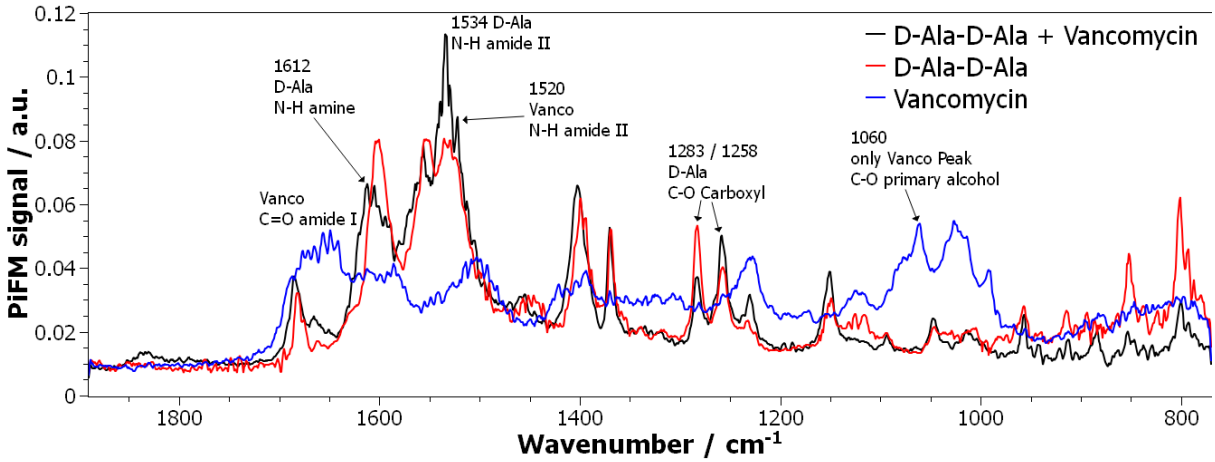


*Figure 6: PiFM interaction analysis of the D-Ala-D-Ala - Vancomycin mixture after 30 minutes reaction time in comparison to pure D-Ala-D-Ala and pure Vancomycin*

The same interaction analysis of the D-Ala-D-Ala and Vancomycin mixture after 30 minutes reaction time in comparison to pure D-Ala-D-Ala and pure Vancomycin was carried out with O-PTIR. For comparative O-PTIR measurements it is firstly required to choose a suitable IR-laser intensity for excitation, that avoids damaging the sample, which was 21% or 47% of maximum IR-laser intensity in this work. Like PiFM, O-PTIR outlines potential interesting spectral regions of the interaction (Fig. 7). This is the N-H amine vibration at 1608 $cm^{-1}$ and the region between 1560 $cm^{-1}$ and 1500 $cm^{-1}$ with N-H and C-N vibrations. Further, there are the C-O carboxyl vibrations at 1284 $cm^{-1}$ and 1260 $cm^{-1}$. Additionally, the C-O primary alcohol vibration at 1060 $cm^{-1}$ from pure Vancomycin this time seems to be also present in the mixture. Maybe resulting from the lower lateral resolution of O-PTIR (≈ 785 nm) compared to PiFM (< 10 nm). While a PiFM spectrum reflects a few nanometers of the interaction surface, O-PTIR spectra are acquired from hundreds of molecules, thereby increasing the probability of measuring pure Vancomycin molecules in the mixture.

All these vibrations are similar to the ones determined with PiFM and are consequently, again, potentially related to the hydrogen bonds, which are involved in the complex formation of D-Ala-D-Ala and Vancomycin.

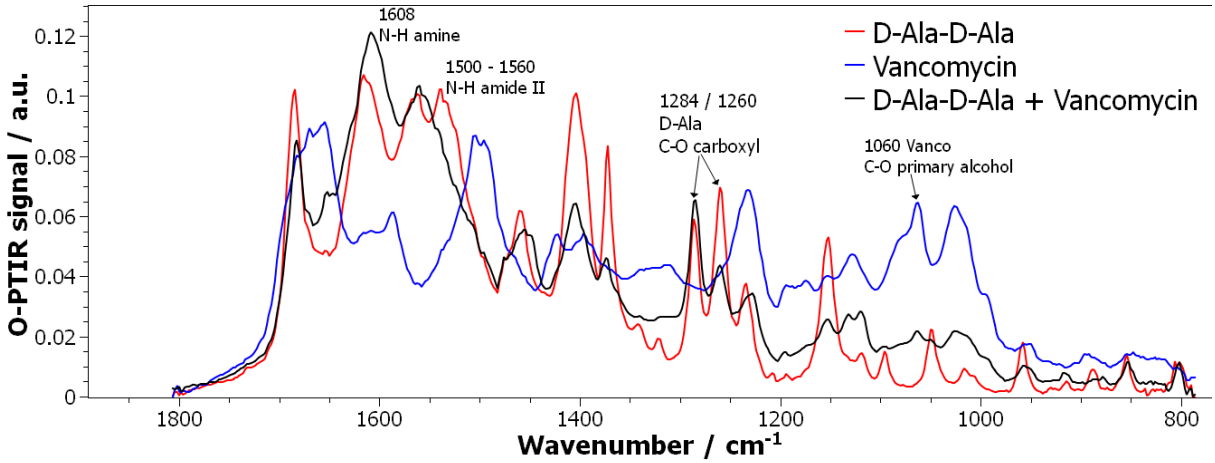


*Figure 7: O-PTIR interaction analysis of the D-Ala-D-Ala - Vancomycin mixture after 30 minutes reaction time in comparison to pure D-Ala-D-Ala and pure Vancomycin*

To further verify the wavenumbers potentially related to the interaction, the second derivatives from PiFM spectra of the D-Ala-D-Ala and Vancomycin mixture, pure D-Ala-D-Ala and pure Vancomycin were compared (Fig. 8). It can be shown that the same N-H amine vibrations as for the PiFM interaction analysis are more prominent in the second derivative of the mixture compared to the pure substances (1608 $cm^{-1}$, 1536 $cm^{-1}$ and 1520 $cm^{-1}$). The N-H vibrational band at 1624 $cm^{-1}$ on the other hand is new compared to the interaction analysis with PiFM but could likewise be related to involved hydrogen bonds. The vibrational bands at 1060 $cm^{-1}$ and in the region of 1680 $cm^{-1}$ to 1640 $cm^{-1}$, which are only present in Vancomycin, can be visualized too, but their intensities are weak. The most prominent vibrations, which are only present in the dipeptide spectra are mainly located in the C-H methyl and C-H alkane regions. Only the peak around 1150 $cm^{-1}$ belongs to a C-O carboxyl vibration and can be associated with hydrogen bonds formed between Vancomycin and D-Ala-D-Ala, since this peak is not present in the mixture.

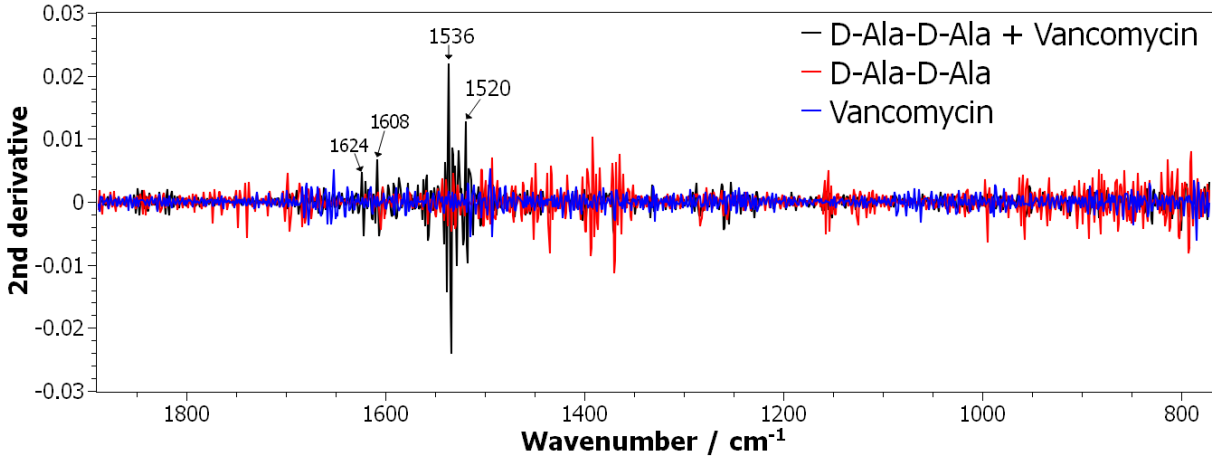


*Figure 8: Second derivatives from PiFM-data of D-Ala-D-Ala - Vancomycin mixture, pure D-Ala-D-Ala and pure Vancomycin*

Based on the interaction wavenumbers (Fig. 6, 8), single wavenumber scans of the D-Ala-D-Ala and Vancomycin mixture were acquired with PiFM for two samples with identical sample preparation. Figure 9a shows the RGB image of the overlayed Scans of the Vancomycin C-O primary alcohol vibrational band at 1060 $cm^{-1}$ (red), the N-H amine vibration involved in the complex formation at 1520 $cm^{-1}$ (green) and 1270 $cm^{-1}$ (blue), which was based on the FTIR spectrum of D-Ala-D-Ala (not shown). Since the PiFM single wavenumber scans must be acquired before the spectra can be measured at selected positions in the scan, it was impossible to recognize that the PiFM spectrum shows no peak at this wavenumber compared to FTIR. Consequently, the blue color reflects just a background peak. Due to that the same experiment was repeated with the C-O carboxyl vibration at 1280 $cm^{-1}$ (blue) as D-Ala-D-Ala peak (Fig. 9b). The single wavenumber scans at 1060 $cm^{-1}$ (red) and 1520 $cm^{-1}$ (green) are the same again. Even if the pixel resolution for the second measurement (Fig. 9b) was increased (≈ 3 nm) in comparison to the first experiment (≈ 4 nm) the instrument performance was not as good as for the first measurement, which shows a clear contrast between green and red. The green regions indicate the presence of pure Vancomycin, while the red color indicates potential interaction sites. In Figure 9b this contrast is only weak and there seems to be much more noise and scan artefacts (horizontal stripes), which reduce the scan quality as well. Due to the fluctuating instrument performance, it is impossible to unambiguously identify local chemical differences within the D-Ala-D-Ala and Vancomycin mixture, because the spatial resolution of PiFM is not sufficient to resolve single interaction complexes, which are probably on the order of 2-3 nm.

a) b)

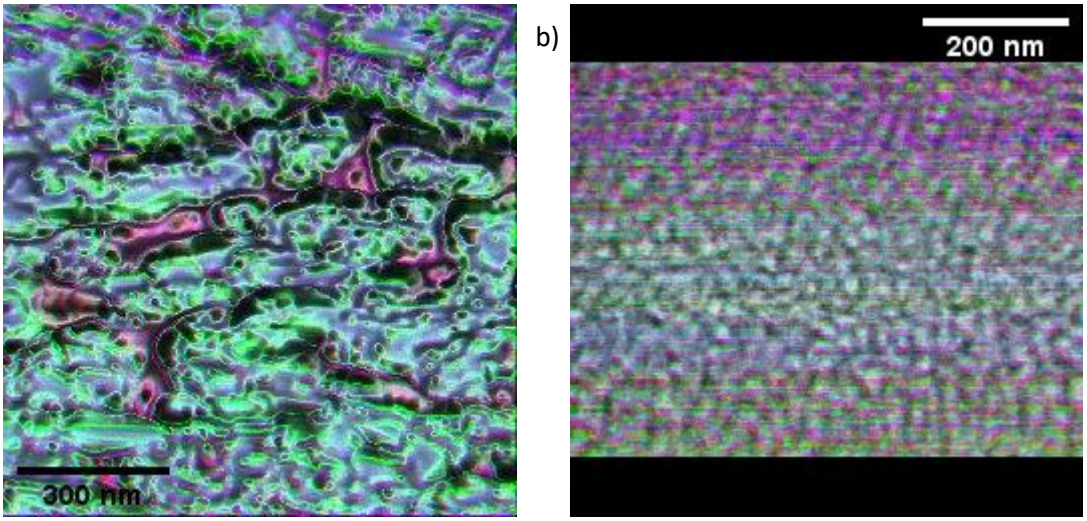


*Figure 9: RGB images of overlayed PiFM single wavenumber scans of D-Ala-D-Ala – Vancomycin mixture from different measurements; (a) overlayed Scans of 1060 $cm^{-1}$ (red), 1520 $cm^{-1}$ (green) and 1270 $cm^{-1}$ (blue); (b) overlayed Scans of 1060 $cm^{-1}$ (red), 1520 $cm^{-1}$ (green) and 1280 $cm^{-1}$ (blue)*

## 4.2 *Bacillus subtilis* – Vancomycin interaction

### 4.2.1 Spectral analysis

To further investigate the interaction of Vancomycin with the bacterial cell wall, the single end group of the peptidoglycan precursor (NAM), the dipeptide D-Ala-D-Ala, was exchanged with the Gram-positive bacterium *Bacillus subtilis*. *Bacillus subtilis* has a thick peptidoglycan layer as main cell wall component and in this way can be affected by the glycopeptide antibiotic Vancomycin (Gilbert *et al.*, 2007; Kahne *et al.*, 2005; Pereira *et al.*, 2007). PiFM spectra of one untreated *Bacillus subtilis* control bacterium (Control30) and two different with Vancomycin treated bacteria (BacVan30) after 30 minutes reaction time, like for the D-Ala-D-Ala and Vancomycin interaction analysis, show the classical vibrational bands of biomolecules. These are, as already explained, from left to right, the amide bands I and II, the C-H methyl vibrations, amide III, C-O sugar vibrations and low intense C-H vibrational bands (Fig. 10). Interestingly, the amide I band between 1700 $cm^{-1}$ and 1600 $cm^{-1}$ in both analyzed treated bacteria is separated into two peaks, while the associated control is missing this division.

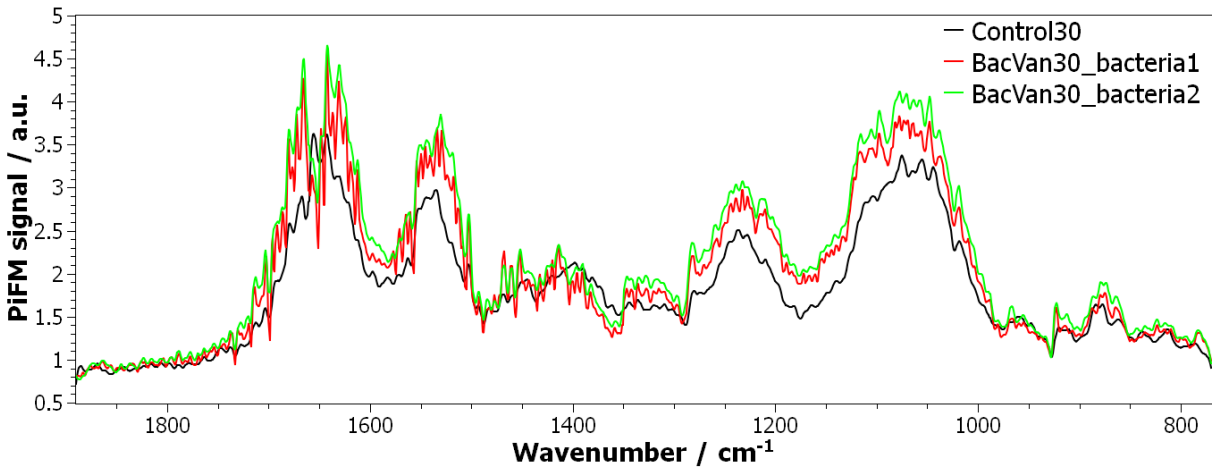


*Figure 10: averaged PiFM spectra of one untreated control bacterium (Control30) and two different with Vancomycin treated bacteria (BacVan30) after 30 minutes reaction time*

Since it is the intention to find differences between BacVan30 and Control30, difference spectra of the analyzed two different with Vancomycin treated bacteria minus the untreated control bacterium were created (Fig. 11). The separation of the amide I band at around 1650 $cm^{-1}$ can be visualized in both difference spectra. Moreover, the same interaction wavenumbers 1612 $cm^{-1}$, 1530 $cm^{-1}$, 1520 $cm^{-1}$ (N-H amine vibrations) and 1283 cm-1 (C-O carboxyl vibration), involved in the hydrogen bond formation for the D-Ala-D-Ala and Vancomycin interaction, can likewise be found. Further differences at 1665 $cm^{-1}$ (C=O ester vibration), 1630 $cm^{-1}$ (N-H amine vibration), 1098 $cm^{-1}$ and 1048 $cm^{-1}$ (C-O carboxyl vibrations) possibly correspond to hydrogen bonds, which are involved in the interaction, too.

However, 1612 $cm^{-1}$ and 1665 $cm^{-1}$ probably represent protein α- and β-helices (Ji *et al.*, 2019). The amide component at 1630 $cm^{-1}$ is most diagnostic for a β-extended, antiparallel-arranged peptide structure and the band near 1100 $cm^{-1}$ is typical for oligo- and polypeptides containing alanine residues, assigned to a combination of C-N and C-C stretching modes (Naumann *et al.*, 1987). Other positive bands in the difference spectra, like for example 1120 $cm^{-1}$, might not be involved, because they are also present in the pure Vancomycin spectrum. Generally, both difference spectra are very similar, only the black spectrum seems to be noisier than the red one. Sharp edges at 1350 $cm^{-1}$ and 1660 $cm^{-1}$ are probably not resulting from chemical differences due to the interaction, because of the QCL laser transitions occurring at these positions.

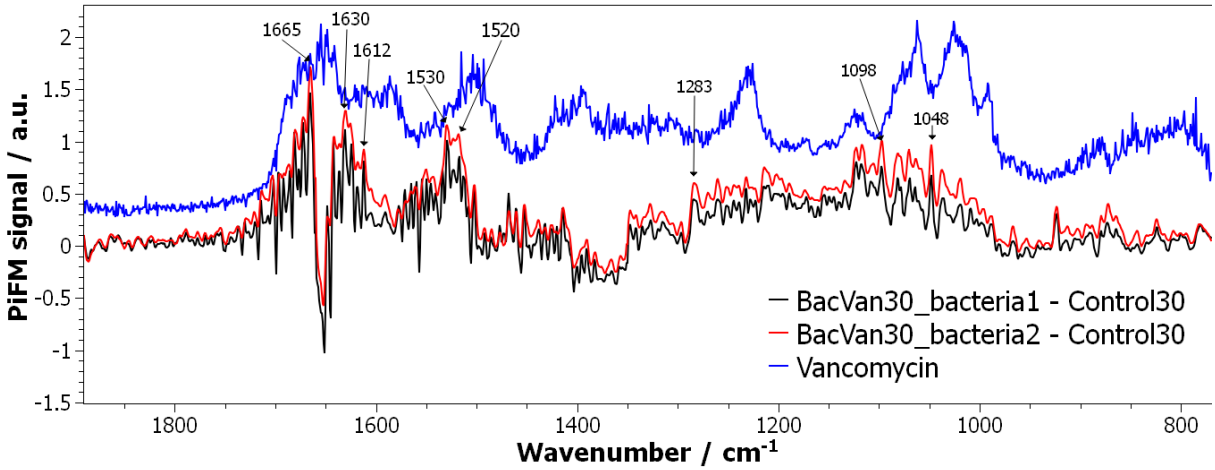


*Figure 11: PiFM difference spectra of two different with Vancomycin treated bacteria (BacVan30) minus the untreated control bacterium (Control30) and pure Vancomycin for comparison*

Especially at these transitions, the interpretation of PiFM results should be handled carefully due to occurring signal dips and at times inhomogeneous excitation of the four QCLs. To this aim it is important to know, where the transitions of the QCLs are. The first transition is located at 1660 $cm^{-1}$, the second one at 1350 $cm^{-1}$ and the last one at 990 $cm^{-1}$. In case of both difference spectra the first and the second transition are visible (Fig. 11). However, inhomogeneous excitation between different QCLs was one of the biggest problems during many measurements, what makes it hard to compare different samples measured at different times or days. The single PiFM spectra of one series of measurements of untreated and treated bacteria at three time points (15, 30 and 60 minutes), exemplary outlines this issue (Fig.12). While the samples Control15, Control30, BacVan30 and BacVan60 look comparable, for the sample BacVan15 the tuner between 1350 $cm^{-1}$ and 990 $cm^{-1}$ has a higher intensity in comparison to the other three QCLs. Completely different laser intensities within and between all four QCL tuners makes it impossible to compare the Control60 spectra with any other sample. Based on this, the focus of this work is on the comparison of treated and untreated bacteria after 30 minutes reaction time (Control30 and BacVan30).

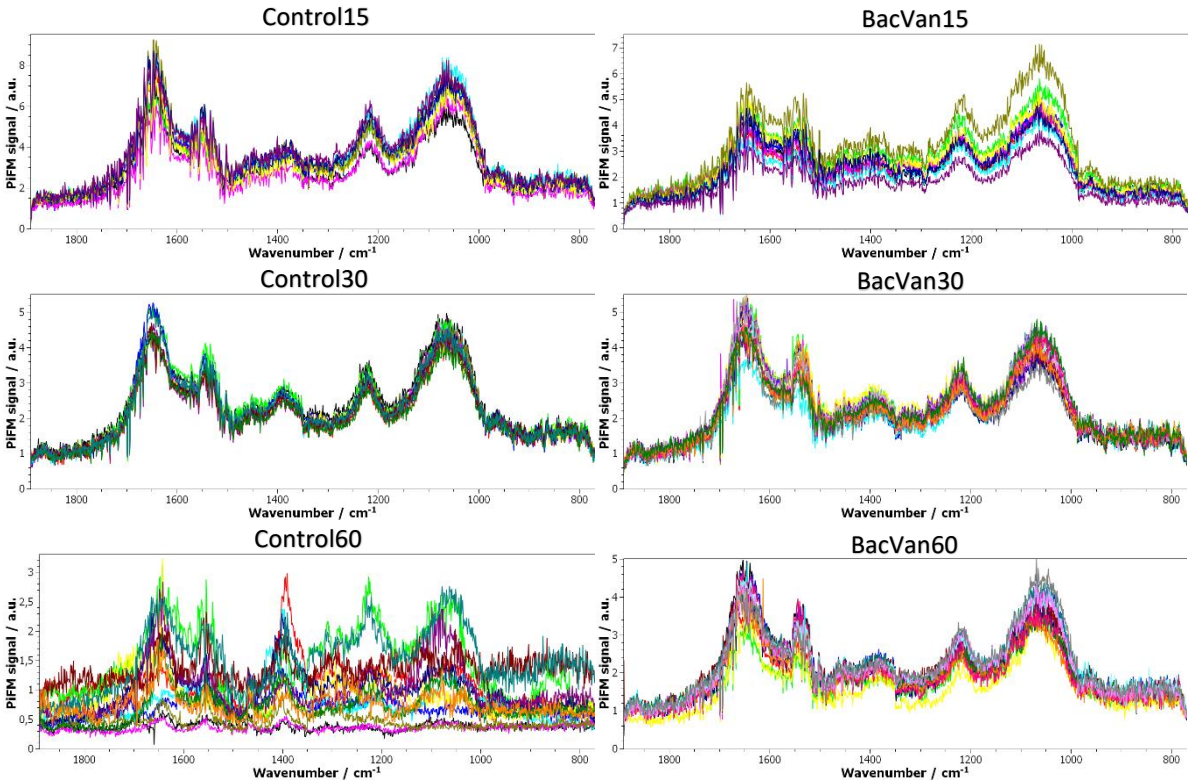


*Figure 12: Single PiFM spectra of one series of measurements of untreated (control) and treated bacteria (BacVan) at three time points (15, 30 and 60 minutes)*

In this way, the further analysis of PiFM spectra of another untreated control bacterium (Control30) and another with Vancomycin treated bacterium (BacVan30) after 30 minutes reaction time show, as expected, the same vibrational bands like in previous measurements (Fig. 10). This time BacVan30 spectra were manually separated in more amide and more sugar rich spectra based on single wavenumber scans at 1060 $cm^{-1}$ (sugar) and 1520 $cm^{-1}$ (amide) (see Fig. 25). Differences between these two groups can already be seen in Figure 13. While the averaged spectra of a more intense amide peak at 1520 $cm^{-1}$ (BacVan30 amide) show higher intensities in all amide bands (I, II and III), the remaining spectra show on average more intense C-O sugar vibrations around 1060 $cm^{-1}$. The corresponding difference spectra of BacVan30, either with amide or with sugar rich spectra minus Control30 likewise show differences especially in the amide regions, but not in the C-O sugar bands (Fig.14). While the difference spectrum with sugar rich spectra does not show many positive difference bands, the difference spectrum with amide rich spectra outlines similar wavenumbers as previously detected (Fig. 11). These are the N-H amine vibrations at 1630 $cm^{-1}$, 1612 $cm^{-1}$, 1542 $cm^{-1}$ and 1520 $cm^{-1}$ and the C-O carboxyl vibration at 1283 $cm^{-1}$. Further differences are at 1669 $cm^{-1}$ (C=O ester vibration) and probably at 1052 $cm^{-1}$ (C-O carboxyl vibration). These results reinforce the assumption that all these vibrational bands are involved in the hydrogen bond formation for the D-Ala-D-Ala and Vancomycin interaction.

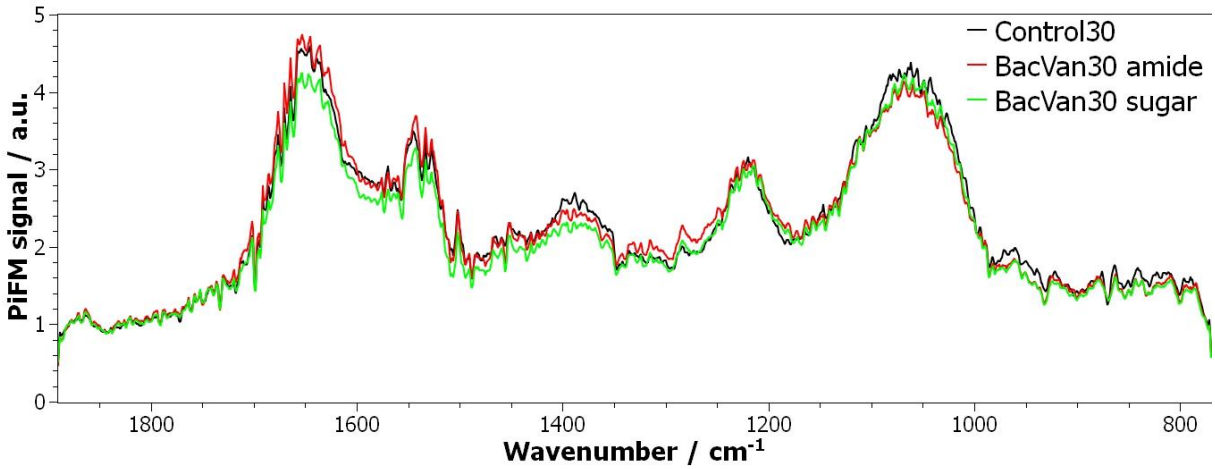


*Figure 13: averaged PiFM spectra of one untreated control bacterium (Control30) and one with Vancomycin treated bacteria (BacVan30) after 30 minutes reaction time; BacVan30 spectra are manually separated in more amide and more sugar rich spectra based on single wavenumber scans of 1060 cm$^{-1}$ (sugar) and 1520 cm$^{-1}$ (amide)*

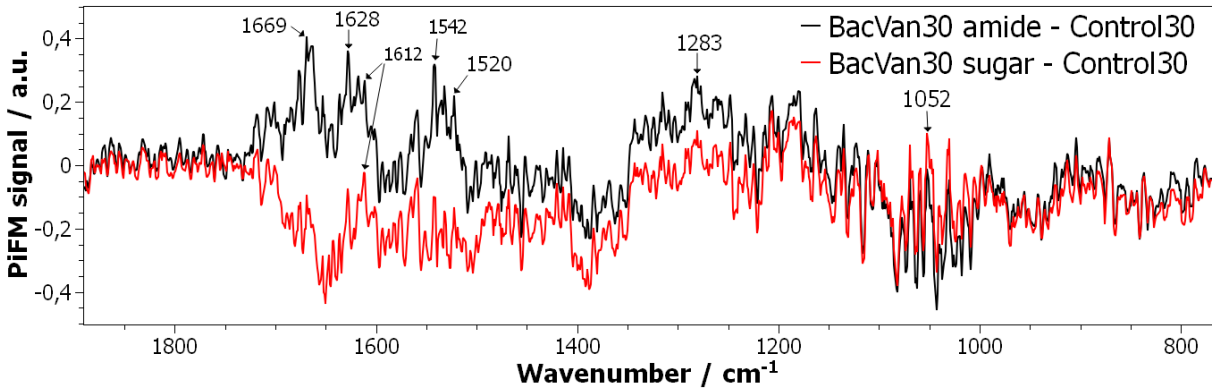


*Figure 14: PiFM difference spectra of with Vancomycin treated bacteria (BacVan30), either with amide or with sugar rich spectra minus the untreated control bacterium (Control30)*

With the lower resolution method, O-PTIR, a complete series of all time points (15, 30 and 60 minutes) of untreated and treated bacteria was measured (Fig. 15). Spectra of all six Control and BacVan samples at various reaction times were further separated into two classes of spectra. The first class represents spectra acquired from single bacteria and small aggregates of bacteria (Fig. 16a). Accumulated bacteria spectra from the edge of the dried drop of the former bacteria solution are incorporated in a second class (Fig 16b). Averaged and normalized O-PTIR spectra of both classes (all Control and BacVan samples) show the same vibrational bands like with PiFM, but it is noticible that the intensity of the amide I band is higher in comparison to the other amide bands and the sugar band.

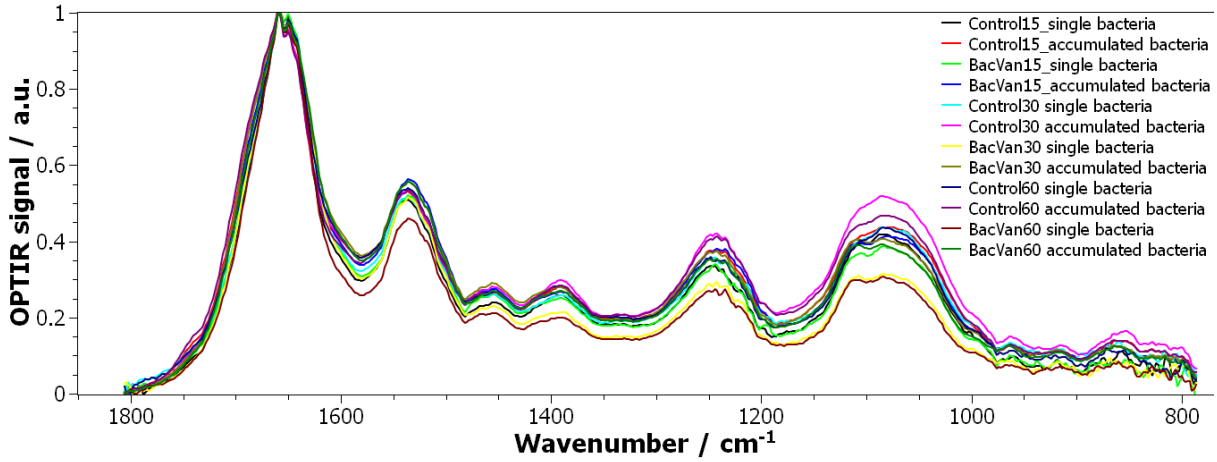


*Figure 15: averaged O-PTIR spectra of untreated control bacteria (Control) and with Vancomycin treated bacteria (BacVan) at three time points (15, 30 and 60 minutes) separated in spectra from single bacteria and accumulated bacteria (see Fig. 16)*

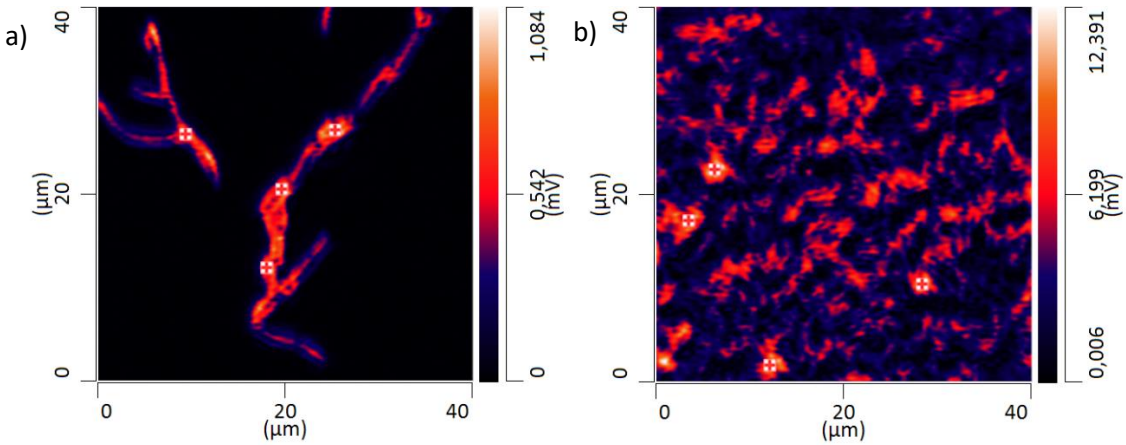


*Figure 16: exemplary O-PTIR single wavenumber maps (1660 cm$^{-1}$) of single (a) and accumulated (b) bacteria from the untreated control sample at 15 minutes (Control15); the markings show exemplary positions where spectra were acquired*

To study the differences between the with Vancomycin treated bacteria and the untreated control, either from single or accumulated bacteria at three time points, difference spectra were also created for the O-PTIR data. It can be shown that the signal-to-noise ratio is better for the difference spectra of the class of accumulated bacteria compared to the single bacteria difference spectra (Fig. 17). Further, the vibrational bands at 1628 $cm^{-1}$, 1520 $cm^{-1}$ (N-H amine) and 1283 $cm^{-1}$ (C-O carboxyl), which seem to be involved in the interaction, can be found for all analyzed samples with O-PTIR, too. However, the peaks in the difference spectra are wider and show no fine structure compared to the PiFM difference spectra (Fig. 11 and 14). Moreover, some negative difference bands could be observed at wavenumbers around 1240 and 1065, except the difference spectra at 15 minutes reaction time, there the intensity of these negative bands is much lower or not pronounced at all. Both negative bands are typical for nucleic acids, which are less produced when the cell differentiation is disturbed by for example the antibiotic Vancomycin (Assmann *et al.*, 2015). Vibrational bands around 1240 $cm^{-1}$ represent a marker for antisymmetric $PO_2^-$ functional group of nucleic acids and around 1065 $cm^{-1}$, there are C-O stretching's of the DNA or RNA backbone (Banyay *et al.*, 2003). These results indicate that the change in the nucleic acid content arises first after 30 minutes reaction time, while changes in the protein content start already after 15 minutes. In this way, it seems logical that Vancomycin first reacts with its target, the peptidoglycan precursor (NAM), such that the complex formation induces changes in the amide bands and after this interaction, the whole cycle of differentiation is disturbed and as a result the nucleic acid biosynthesis is reduced. Due to the bigger depth cross-section from where the O-PTIR signal is acquired (hundreds of nm up to a few mm), nucleic acid changes can be detected with O-PTIR, but not with PiFM (Douplik *et al.*, 2013; Padalkar & Pleshko, 2015). PiFM is a surface sensitive method, where the photo-induced force is in a range of 2 - 10 nm (MolecularVista, 2021; Otter *et al.*, 2021).

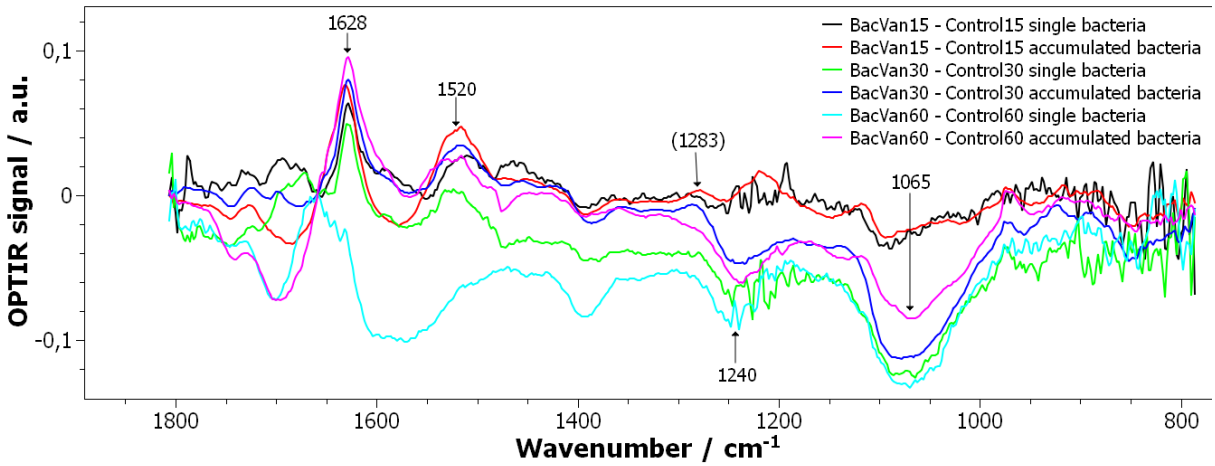


*Figure 17: O-PTIR difference spectra of with Vancomycin treated bacteria (BacVan) minus untreated control bacteria (Control), either from single or accumulated bacteria at three time points (15, 30 and 60 minutes)*

For comparison, also FTIR difference spectra of with Vancomycin-treated bacteria minus untreated control bacteria at three time points (15, 30 and 60 minutes) were analyzed. The samples at 15 minutes reaction time had a bad signal-to-noise ratio and water vapor artefacts, so that it was impossible to detect any differences in the difference spectrum (not shown). The difference spectra at 30 and 60 minutes show the same negative bands around 1240 $cm^{-1}$ and 1065 $cm^{-1}$, which are associated with nucleic acid changes. Furthermore, the N-H vibration around 1626 $cm^{-1}$ and the C-O carboxyl band at 1283 $cm^{-1}$ can be found, but the change in the amide II band around 1520 $cm^{-1}$ is missing compared to O-PTIR.

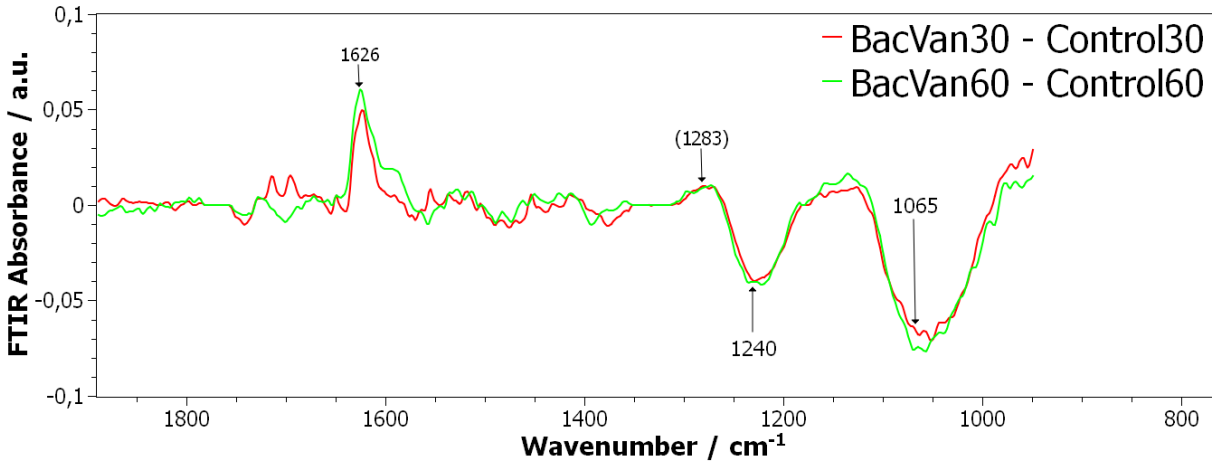


*Figure 18: FTIR difference spectra of with Vancomycin treated bacteria (BacVan) minus untreated control bacteria (Control) at two time points (30 and 60 minutes)*

### 4.2.2 Principal component analysis (PCA) of single spectra

The aim of the PCA was to test, if it is possible to separate the single spectra of untreated and with Vancomycin-treated bacteria with an undirected statistical method without further data pre-processing, except scaling with the excitation intensity. The PCA results of two independent PiFM measurements of single spectra from Control30 and BacVan30 show for both measurement series a clear separation of the control and treated spectra (Fig. 19). This separation is mainly based on the second principal component (PC2), which has differential features in the C-O sugar band region around 1060 $cm^{-1}$ and between 1450 $cm^{-1}$ and 1375 $cm^{-1}$ (C-H methyl vibrations) compared to the first principal component (PC1). Control30 spectra 5 and 6 of the first measurement series seem to be outliers, probably due to a different signal-to-noise ratio.

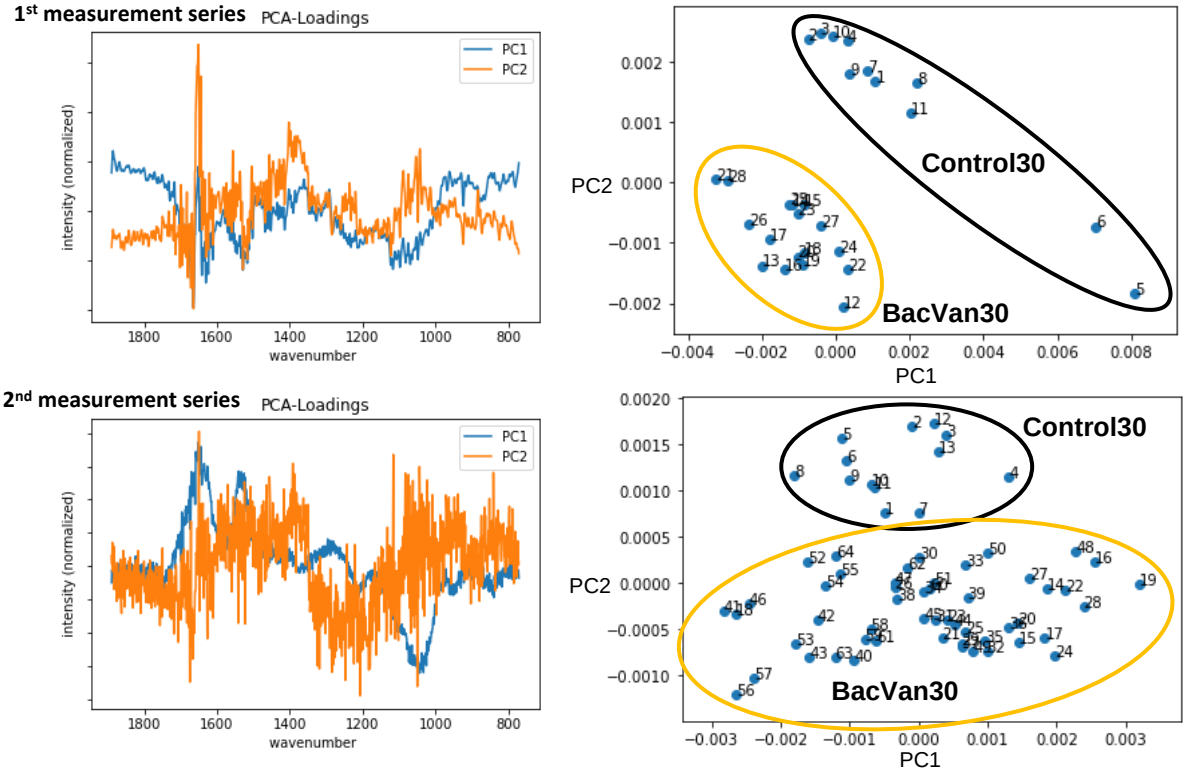


*Figure 19: PCA results of two independent PiFM measurements of single spectra from untreated (Control30) and treated bacteria (BacVan30) at 30 minutes reaction time; the left plots show the Loadings of the PCA, and the associated scatterplots are shown on the right*

The same PCA was carried out for O-PTIR measurements of single spectra from untreated and treated bacteria at 30 minutes reaction time from both, single and accumulated bacteria. A separation of Control30 and BacVan30 can likewise be observed (Fig. 20). This time it seems that the separation is not only based on differential features of PC2, which are the C-O sugar vibrations around 1060 $cm^{-1}$ and the amide III band around 1220 $cm^{-1}$ compared to PC1. Possibly a third principal component is needed to find features, which explain the separation of the control and treated single spectra. Furthermore, a diagonal separation of single and accumulated bacteria samples can be shown in the scatterplot for the measurements at 30 minutes reaction time (Fig. 20). These diagonal separation of single and accumulated bacteria spectra is likewise observed for the PCA results of O-PTIR measurements from untreated and treated bacteria at all three time points (Fig. 21).

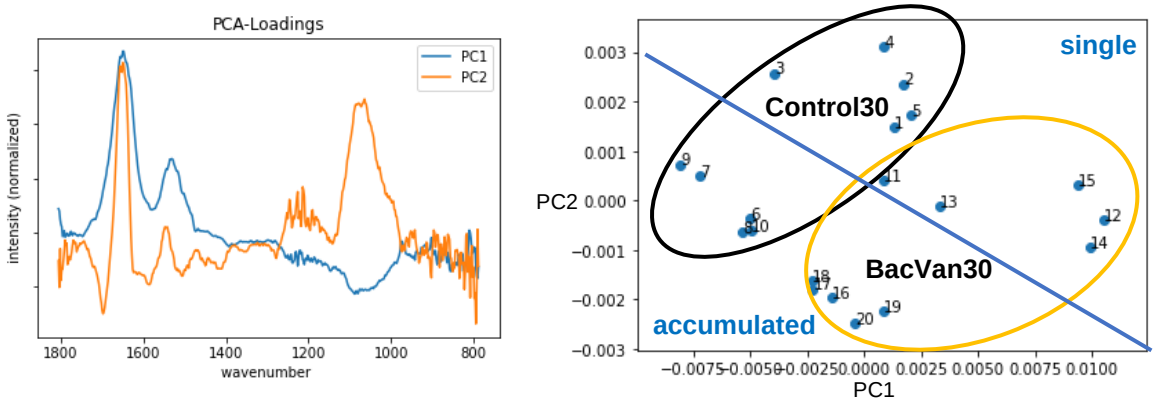


*Figure 20: PCA results of O-PTIR measurements of single spectra from untreated (Control30) and treated bacteria (BacVan30) at 30 minutes reaction time from both, single and accumulated bacteria; the left plot shows the Loadings of the PCA, and the associated scatterplot is shown on the right*

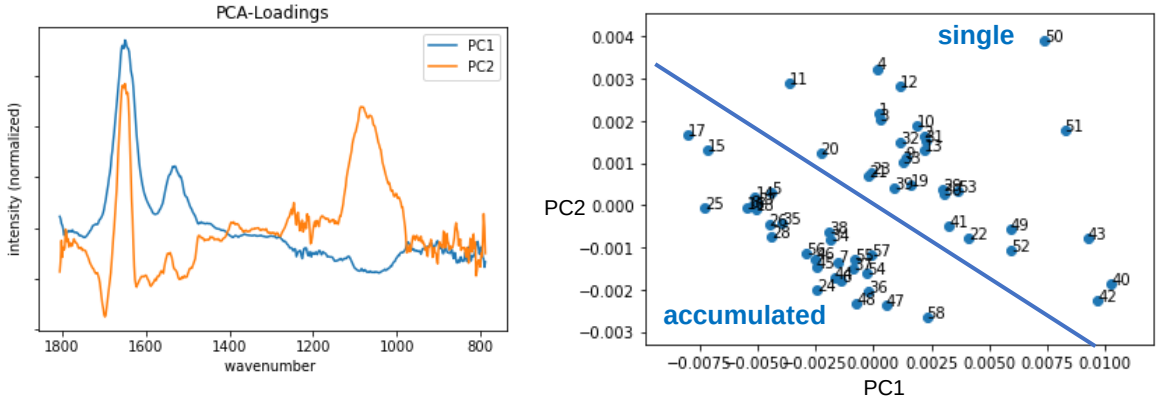


*Figure 21: PCA results of O-PTIR measurements of single spectra from untreated (Control) and treated bacteria (BacVan) at three time points (15, 30 and 60 minutes reaction time) from both, single and accumulated bacteria; the left plot shows the Loadings of the PCA, and the associated scatterplot is shown on the right*

Due to no clearly visible separation of Control and BacVan spectra from both, single and accumulated bacteria, also a PCA of only accumulated bacteria at 15, 30 and 60 minutes was carried out. The results show a separation of accumulated Control and BacVan spectra, which differential features, again, can not only be explained with PC1 and PC2. PC2 explains only a part of the differential features, which are around 1100 $cm^{-1}$ and 1670 $cm^{-1}$ compared to PC1.

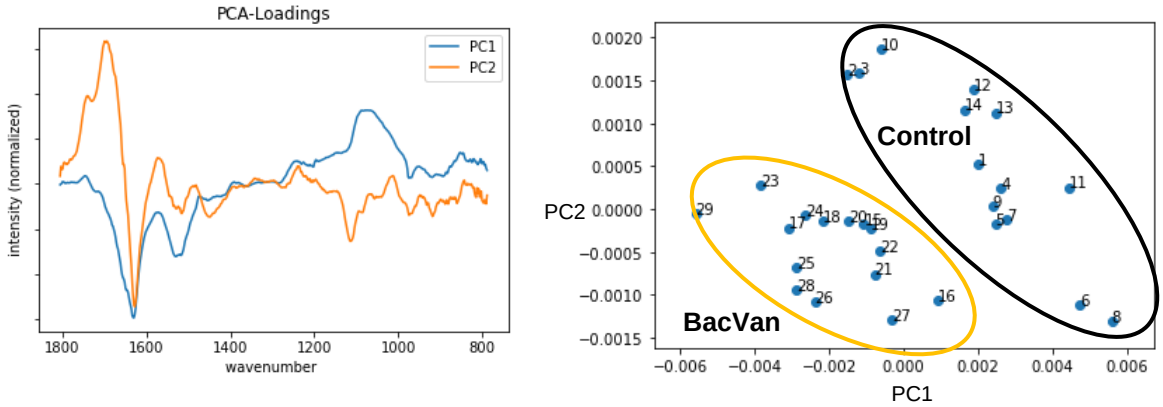


*Figure 22: PCA results of O-PTIR measurements of single spectra from untreated (Control) and treated bacteria (BacVan) at three time points (15, 30 and 60 minutes reaction time) only from accumulated bacteria; the left plot shows the Loadings of the PCA, and the associated scatterplot is shown on the right*

### 4.2.3 Imaging analysis

To study the interaction of Vancomycin with the bacterial cell wall of the Gram-positive bacterium *Bacillus subtilis*, single wavenumber scans of wavenumbers potentially involved in the hydrogen bond formation between Vancomycin and the D-Ala-D-Ala end group of the peptidoglycan precursor (NAM) were accomplished. But before, the different scan modes of PiFM were tested with single wavenumber scans of an untreated bacterium at 15 minutes at the interaction-based wavenumber 1612 $cm^{-1}$ with a pixel resolution of ≈ 8 nm. In the so called PiF-mode the detection frequency of the photo-induced force is determined manually only once before the complete scan is acquired (Fig. 23a). PiFM-mode enables a determination of the detection frequency of the photo-induced force before each pixel of the scan is measured (Fig. 23b). This is also the crucial difference between both modes, since the detected signal collapses in PiF-mode if a substance measured at any position has different mechanical properties (e. g. softness) compared to the region, where the initial detection frequency was determined. In this way further scans were acquired in PiFM-mode.

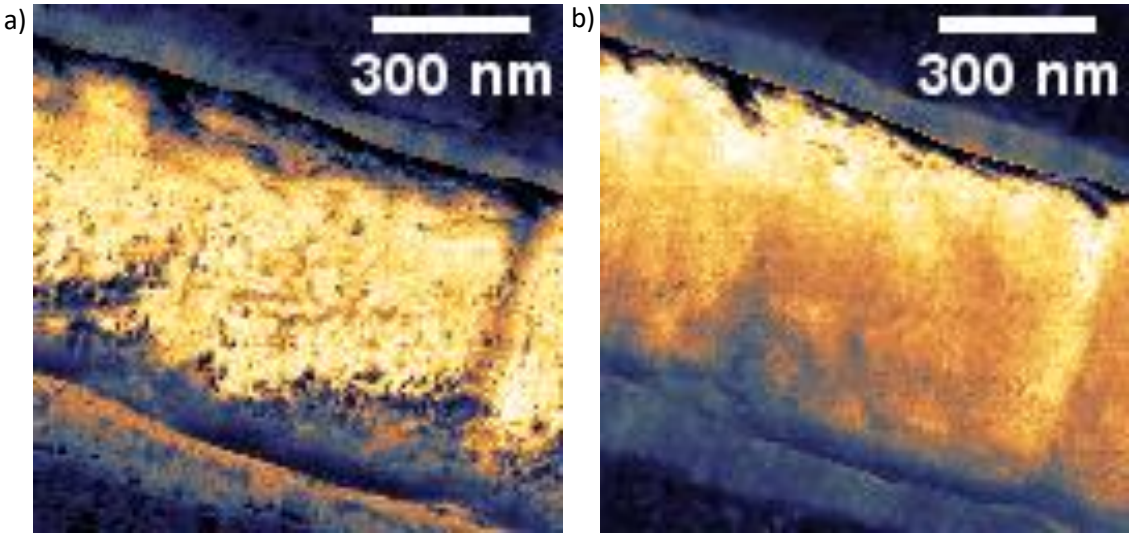


*Figure 23: PiFM single wavenumber (zoom) scans of an untreated bacterium at 15 minutes of the interaction-based wavenumber 1612 $cm^{-1}$ acquired with (a) PiF-mode (b) PiFM-mode*

For visualization of the interaction of Vancomycin with *Bacillus subtilis*, the single wavenumber scans were combined as RGB images. Based on the previous results of the D-Ala-D-Ala and Vancomycin, respectively, the *Bacillus subtilis* and Vancomycin interaction analysis, the interaction-based wavenumbers 1520 and 1612 were chosen to represent changes in the amide I and II bands (N-H amine vibrations). 1060 $cm^{-1}$ was selected to visualize sugar bands (C-O carboxyl vibration) of the bacteria and probably show pure, not reacted Vancomycin.

The RGB image of overlayed PiFM single wavenumber scans with a pixel resolution of ≈ 20 nm of Control30 at 1060 $cm^{-1}$ (blue + red) and 1520 $cm^{-1}$ (green) shows horizontal stripes, which is a frequent PiFM scan artefact probably caused by soft substances collected from the sharp tip. Attached to the tip these substances can cause such horizontal stripes as observed in Figure 24 and due to the used tapping mode, the tip can get rid of this contamination comparatively fast. Moreover, in the control sample there is no color contrast visible at potential division sites of the bacteria. The combination of the blue and red color was used to get a better visualized contrast with green.

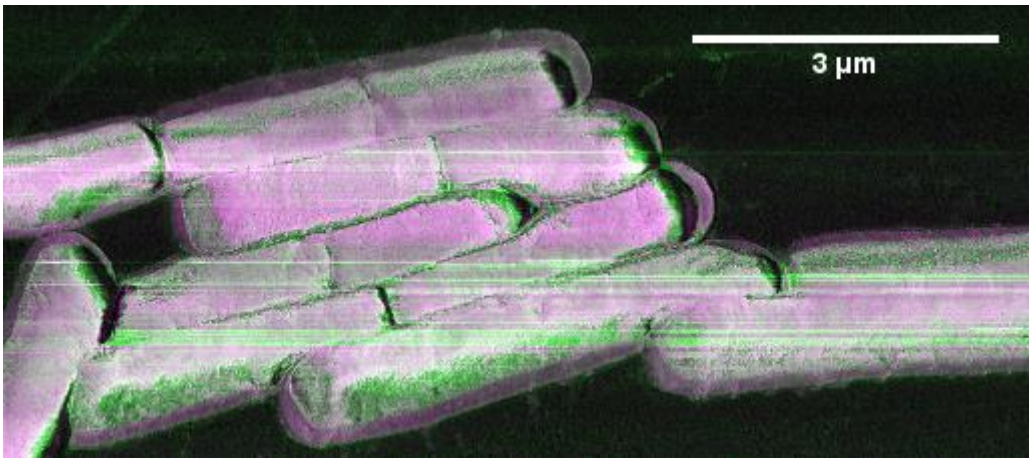


*Figure 24: RGB image of overlayed PiFM single wavenumber scans of untreated control at 30 minutes of the sugar and Vancomycin peak 1060 $cm^{-1}$ (blue + red) and the interaction-based wavenumber 1520 $cm^{-1}$ (green)*

The same RGB image of overlayed PiFM single wavenumber scans with a pixel resolution of ≈ 20 nm of BacVan30 at 1060 $cm^{-1}$ (blue + red) and 1520 $cm^{-1}$ (green) on the other hand shows clearly visible green regions close to potential division sites of the with Vancomycin treated bacteria marked with the yellow arrows (Fig. 25). To further analyze these regions more high-resolution scans with a pixel resolution of ≈ 4 nm of the square marked region were measured. The overlayed PiFM scans of the sugar and Vancomycin peak at 1060 $cm^{-1}$ (blue + red) and the interaction-based wavenumber 1520 $cm^{-1}$ (green) in figure 26a visualizes a clear green contrast. This contrast suggests a binding of Vancomycin and a following complexation of the peptidoglycan precursor (NAM), which is increasingly being released if cell division is initiated, and a new cell wall must be built up. As a result of the Vancomycin action cell differentiation is disturbed and leakage of the bacterium at the division site can be observed, like in the lower right corner (Fig. 26a). If also the second interaction-based wavenumber 1612 (green) is overlayed with the scans of the sugar and Vancomycin peak 1060 $cm^{-1}$ (blue) and the other interaction-based wavenumber 1520 $cm^{-1}$ (red), the same contrast in yellow, the mixed color of green and red, can be observed (Fig. 26b). This further clarifies the highly localized action of Vancomycin at division sites of the *Bacillus subtilis* samples.

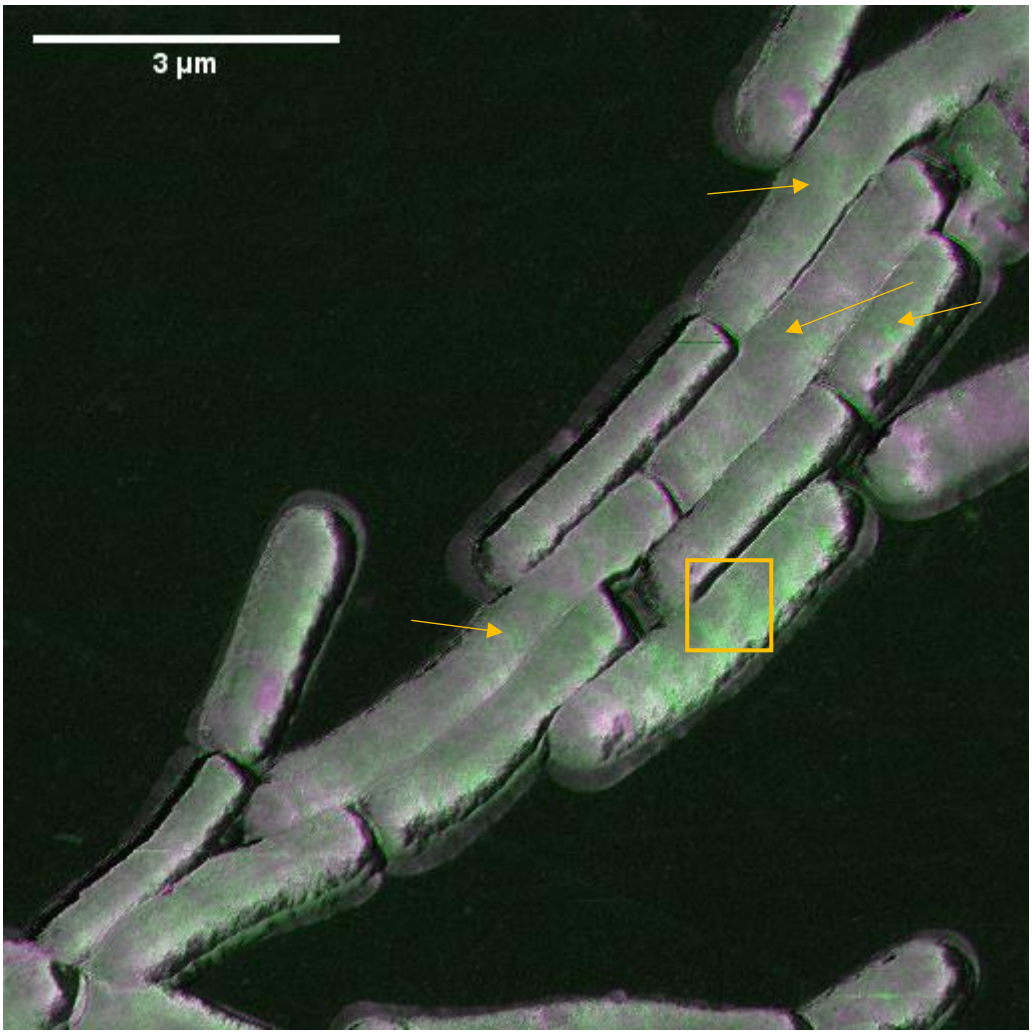


*Figure 25: RGB image of overlayed PiFM single wavenumber scans of Vancomycin-treated bacteria after 30 minutes reaction time of the sugar and Vancomycin peak 1060 $cm^{-1}$ (blue + red) and the interaction-based wavenumber 1520 $cm^{-1}$ (green)*

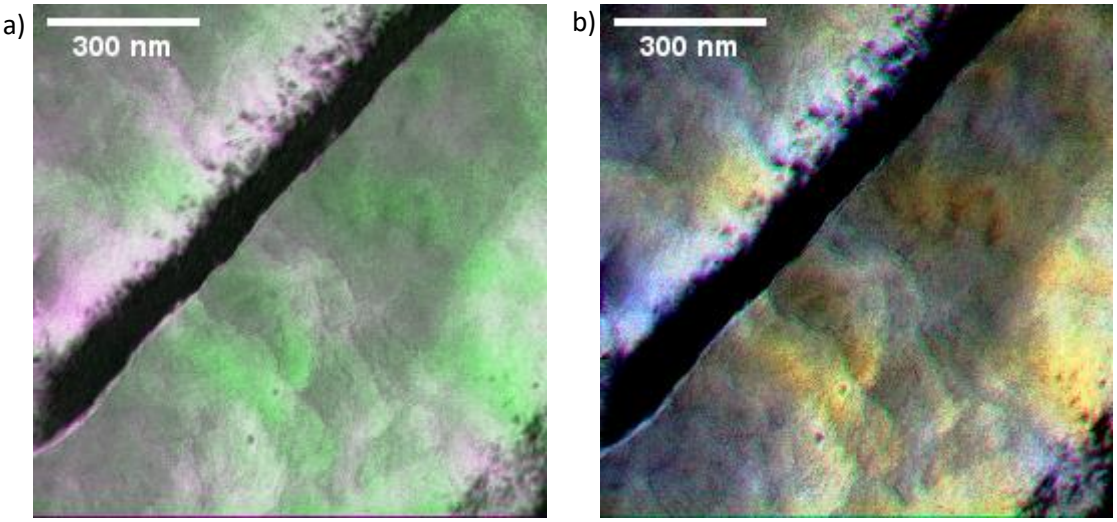


*Figure 26: RGB images of overlayed PiFM single wavenumber (zoom) scans of Vancomycin-treated bacteria after 30 minutes reaction time of (a) the sugar and Vancomycin peak 1060 $cm^{-1}$ (blue + red) and the interaction-based wavenumber 1520 $cm^{-1}$ (green) and (b) the sugar and Vancomycin peak 1060 $cm^{-1}$ (blue) and the interaction-based wavenumbers 1520 $cm^{-1}$ (red) and 1612 $cm^{-1}$ (green)*

Additionally, comparable RGB images of overlayed PiFM single wavenumber scans with a pixel resolution of ≈ 4 nm of BacVan60 at 1060 $cm^{-1}$ (blue + red) and 1520 $cm^{-1}$ (green) in figure 27a and 1060 $cm^{-1}$ (blue), 1520 $cm^{-1}$ (red) and 1612 $cm^{-1}$ (green) in figure 27b show similar green or yellow contrasts compared to BacVan30. For the overlayed PiFM single wavenumber scans of the untreated bacteria sample (BacVan15) at 1060 $cm^{-1}$ (blue), 1520 $cm^{-1}$ (red) and 1612 $cm^{-1}$ (green), however, this contrast at potential division sites is missing (Fig. 28). This observation suggests that the action of Vancomycin is not yet so pronounced after 15 minutes reaction time like after 30 and 60 minutes.

a) b)

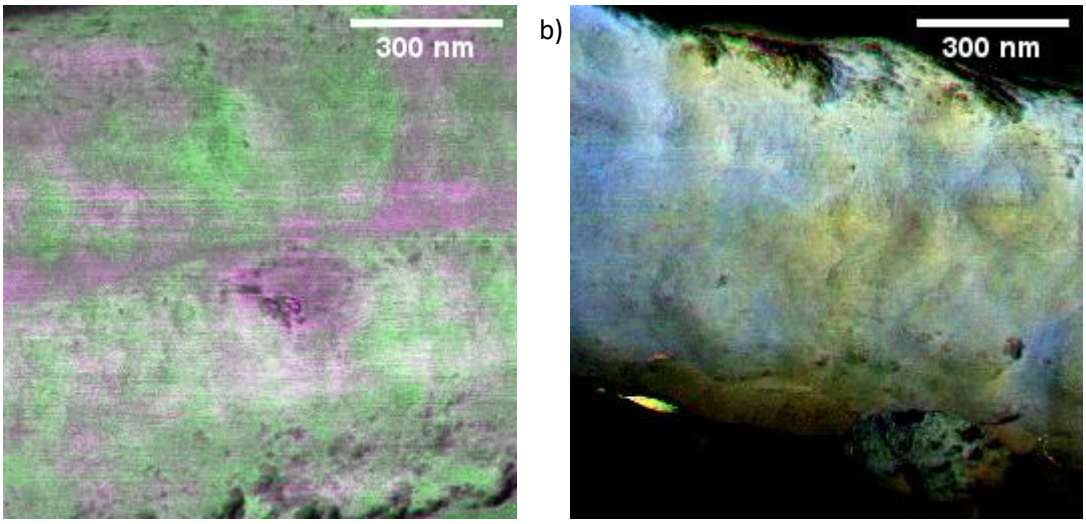


*Figure 27: RGB images of overlayed PiFM single wavenumber (zoom) scans of two different Vancomycin-treated bacteria after 60 minutes reaction time of (a) the sugar and Vancomycin peak 1060 $cm^{-1}$ (blue + red) and the interaction-based wavenumber 1520 $cm^{-1}$ (green) and (b) the sugar and Vancomycin peak 1060 $cm^{-1}$ (blue) and the interaction-based wavenumbers 1520 $cm^{-1}$ (red) and 1612 $cm^{-1}$ (green)*

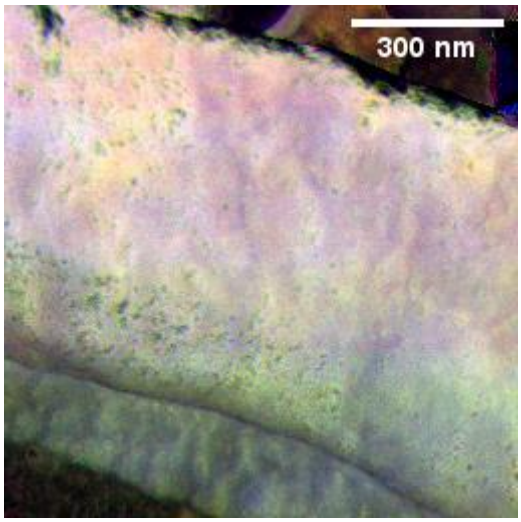


*Figure 28: RGB images of overlayed PiFM single wavenumber (zoom) scans of Vancomycin-treated bacteria after 15 minutes reaction time of the sugar and Vancomycin peak 1060 $cm^{-1}$ (blue) and the interaction-based wavenumbers 1520 $cm^{-1}$ (red) and 1612 $cm^{-1}$ (green)*

To study the possibilities of O-PTIR to visualize the interaction of Vancomycin with the bacterial cell wall of the Gram-positive bacterium *Bacillus subtilis*, single wavenumber maps of wavenumbers potentially involved in the hydrogen bond formation between Vancomycin and the D-Ala-D-Ala end group of the peptidoglycan precursor (NAM) were accomplished, too. To this aim, the most intense wavenumbers (see Fig. 15) were used to get the best possible intensities. 1668 (C=O esters vibration) and 1536 (N-H amine vibration) were chosen to represent the amide I and II bands and 1080 $cm^{-1}$ (C-O carboxyl vibration) was selected to visualize sugar bands of the bacteria. But the RGB image of overlayed O-PTIR single wavenumber maps with a pixel resolution of 1 µm of Vancomycin-treated bacteria after 15 minutes reaction time shows that it is impossible to even see how many bacteria are visible in the image due to the much lower spatial resolution of O-PTIR compared to PiFM (Fig. 29). In this way O-PTIR is not able to image the highly localized action of Vancomycin at division sites of the *Bacillus subtilis* samples.

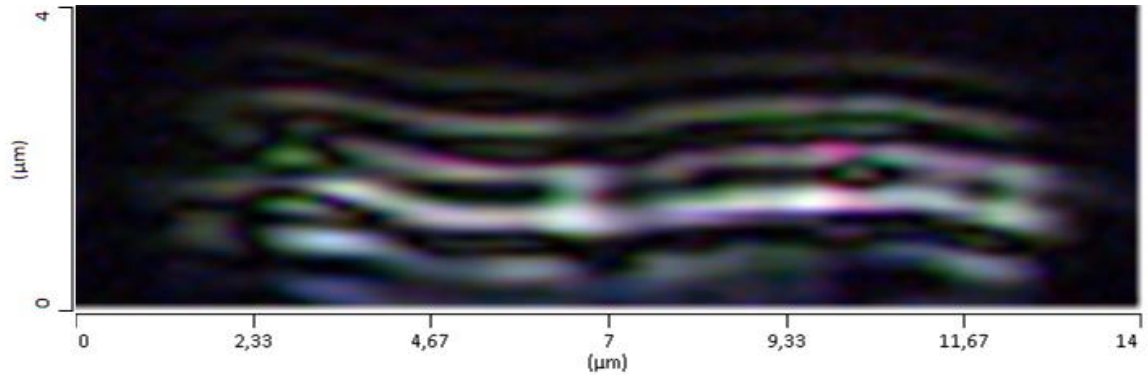


*Figure 29: RGB image of overlayed O-PTIR single wavenumber maps of Vancomycin-treated bacteria after 15 minutes reaction time of the sugar peak 1080 $cm^{-1}$ (blue) and the amide vibrations at 1536 $cm^{-1}$ (red) and 1668 $cm^{-1}$ (green)*

### 4.2.4 Hyperspectral scan analysis

Since PiFM single wavenumber scans are limited to the information content of one selected wavenumber, hyperspectral scans enable the analysis of a whole spectrum or a decent wavenumber region. Due to the occurring inhomogeneous excitation of the four QCLs, PiFM hyperspectral scans were acquired only inside one QCL tuner. A pixel resolution of ≈ 28 nm was chosen because of the long measurement times of about 28 hours per hyperspectral scan, if only one complete QCL tuner is analyzed. Based on the previous results of the *Bacillus subtilis* and Vancomycin interaction analysis the third tuner between 1349 $cm^{-1}$ and 990 $cm^{-1}$ and the second tuner from 1659 $cm^{-1}$ to 1350 $cm^{-1}$ were selected for the hyperspectral scans, since these tuners cover the main interaction-based wavenumbers, which are probably involved in the hydrogen bond formation. Due to the huge amount of data generated with hyperspectral scanning, PCA was used to find differences within these broad spectral regions. The PCA results of a hyperspectral PiFM scan of a with Vancomycin-treated bacterium after 30 minutes reaction time within a range from 1350 $cm^{-1}$ to 1659 $cm^{-1}$ shows a contrast in the factor plot of PC1, which might result from real chemical features (Fig. 30). The difference in the contrast of the factor plots of PC1 and PC2 is possibly based on differences in the amide II content between 1560 $cm^{-1}$ and 1510 $cm^{-1}$. The contrast of the factor plots of PC2 and PC3 could be caused by chemical differences within the C-H methyl vibrational region around 1420 $cm^{-1}$ and a specific amide II band at 1508 $cm^{-1}$.

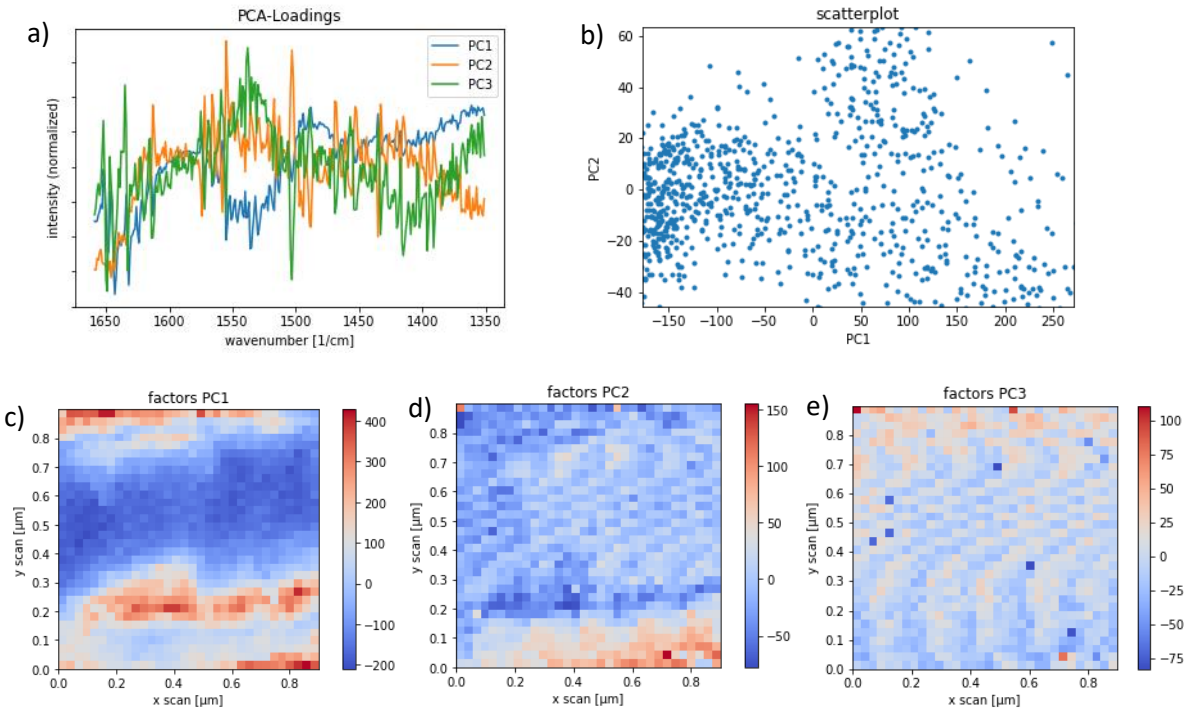


*Figure 30: PCA results of a hyperspectral PiFM scan of with Vancomycin treated bacterium after 30 minutes reaction time within a range from 1350 to 1659 $cm^{-1}$; (a) PCA loadings; (b) associated scatterplot; (c-e) factor plots*

The PCA results of the hyperspectral PiFM scan from the same sample region of the same with Vancomycin-treated bacteria sample after 30 minutes reaction time within a range of 990 $cm^{-1}$ to 1349 $cm^{-1}$ outlines a similar contrast in the factor plot of PC1 as for the second tuner. This contrast is probably based on differences in the C-O carboxyl vibration at 1283 $cm^{-1}$ (Fig. 31). This result suggests that the contrast in both factor plots of PC1 is consistently based on differences within the interaction-based wavenumbers around amide II and C-O carboxyl vibrational bands. To compare the factor plots of PC2 and PC3, a modification within the used in-house python program (HyPIRana) is needed to exclude single abnormal pixels or complete lines, which was not yet completed during this work. Moreover, other multivariant statistical analyses, like hierarchical clustering or topological data analysis (TDA) might be able to further promote the understanding of chemical differences within and between the different hyperspectral data sets.

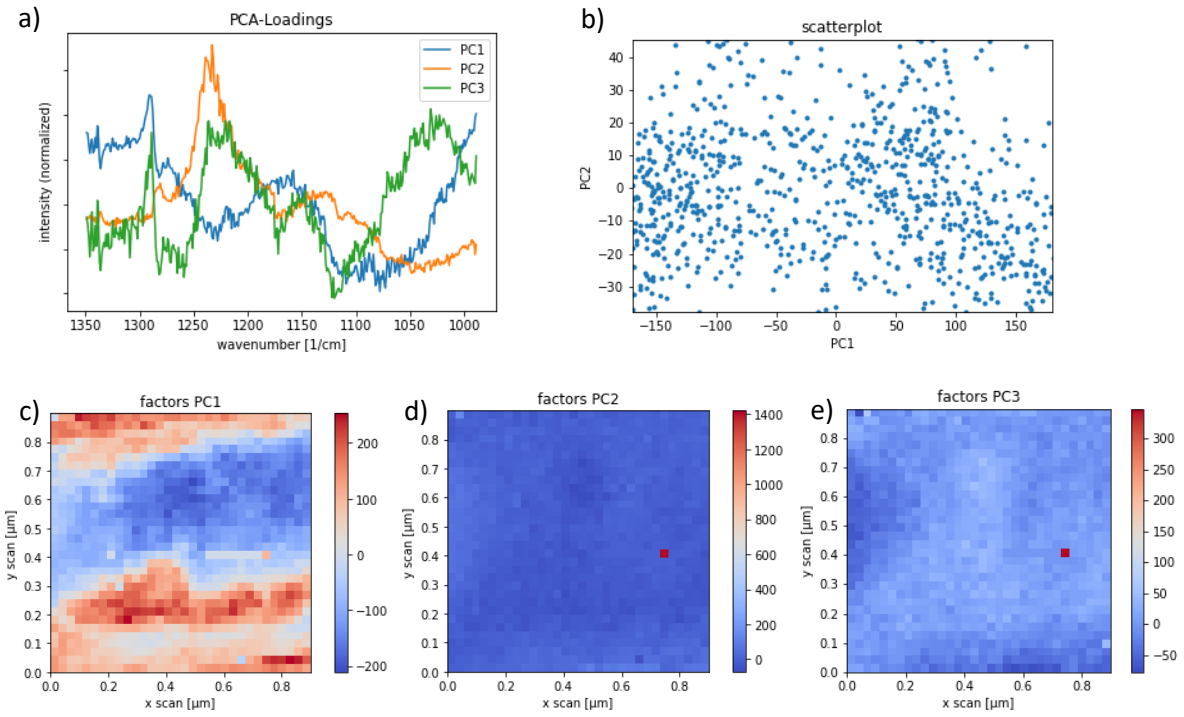


*Figure 31: PCA results of a hyperspectral PiFM scan of with Vancomycin treated bacterium after 30 minutes reaction time within a range from 990 to 1349 $cm^{-1}$; (a) PCA loadings; (b) associated scatterplot; (c-e) factor plots*

# 5 Summary

To study the interaction of Vancomycin with the bacterial cell wall, first the single end group of the peptidoglycan precursor (NAM), the dipeptide D-Ala-D-Ala, was used. Generally, due to the lower wavenumber resolution of PiFM (1 $cm^{-1}$) compared to O-PTIR and FTIR (2 $cm^{-1}$) and the higher spatial resolution, PiFM is likewise superior to the other methods in relation to spectral resolution. However, both new methods O-PTIR and PiFM enable the detection of vibrations within the amide I, II and III bands and the C-O carboxyl region, which are probably related to hydrogen bonds, involved in the complex formation of D-Ala-D-Ala and Vancomycin. If the single end group of the peptidoglycan precursor (NAM), the dipeptide D-Ala-D-Ala, is exchanged with the Gram-positive bacterium *Bacillus subtilis* similar interaction-based vibrations within the amide I, II and III bands and the C-O carboxyl region can be found. Moreover, PCA enables the separation of single spectra from untreated and with Vancomycin-treated bacteria without further data pre-processing for O-PTIR and PiFM. Even if the sub-10 nm spatial resolution of PiFM is not sufficient to resolve single interaction complexes, which are probably on the order of 2-3 nm, it is possible to visualize the binding of Vancomycin and a following complexation of the peptidoglycan precursor (NAM) with so called PiFM-mode. NAM is increasingly being released when cell division is initiated, and a new cell wall must be built up. As a result of the highly localized Vancomycin action, cell differentiation is disturbed and leakage of the bacterium at the division site can be observed with PiFM. Furthermore, the results of this work suggest that the action of Vancomycin is not yet so pronounced after 15 minutes reaction time as after 30 and 60 minutes. With O-PTIR, respectively, it is impossible to find out how many bacteria are visible in an RGB image of overlayed single wavenumber maps due to the much lower spatial resolution of O-PTIR compared to PiFM. In this way O-PTIR is not able to image the highly localized action of Vancomycin at division sites of the *Bacillus subtilis* samples. Since PiFM single wavenumber scans are limited to the information content of one selected wavenumber, hyperspectral scans enable the analysis of a whole spectrum or a decent wavenumber region. The PCA results of the hyperspectral data suggest that the visualized contrast might be based on differences within the interaction-based wavenumbers around amide II and C-O carboxyl vibrational bands. To further promote the understanding of chemical differences within and between the PiFM hyperspectral data sets, single wavenumber scans and complete spectra, an improved calibration of the IR-laser intensity of the four QCLs is needed due to occurring signal dips and at times inhomogeneous excitation. Additionally, one specific laser over the entire range of amide I and II bands or even all amide and C-O carboxyl vibrational bands might be useful.

# List of figures

# References


Aktories K., Förstermann U., Starke K., Hofmann F.B. (2017) *Allgemeine und spezielle Pharmakologie und Toxikologie: Begründet von W. Forth, D. Henschler, W. Rummel*: Elsevier Health Sciences.

Assmann C., Kirchhoff J., Beleites C., Hey J., Kostudis S., Pfister W., Schlattmann P., Popp J., Neugebauer U. (2015) Identification of vancomycin interaction with Enterococcus faecalis within 30 min of interaction time using Raman spectroscopy. *Analytical and bioanalytical chemistry*, **407**, 8343–8352.

Baden N., Kobayashi H., Urayama N. (2020) Submicron-resolution polymer orientation mapping by optical photothermal infrared spectroscopy. *International Journal of Polymer Analysis and Characterization*, **25**, 1–7.

Badger S. (2017) Raman Imaging and Mapping. URL https://blue-scientific.com/raman-imaging-mapping/.

Baker M., Hughes C., Hollywood K. (2016) *Biophotonics: Vibrational Spectroscopic Diagnostics.* 1st edn. Bristol: IOP Concise Physics - A Morgan & Claypool Publication.

Banyay M., Sarkar M., Gräslund A. (2003) A library of IR bands of nucleic acids in solution. *Biophysical chemistry*, **104**, 477–488.

Burkard M., Stein T. (2008) Microtiter plate bioassay to monitor the interference of antibiotics with the lipid II cycle essential for peptidoglycan biosynthesis. *Journal of microbiological methods*, **75**, 70–74.

Cristie-David A.S., Chen J., Nowak D.B., Bondy A.L., Sun K., Park S.I., Banaszak Holl M.M., Su M., Marsh E.N.G. (2019) Coiled-coil-mediated assembly of an icosahedral protein cage with extremely high thermal and chemical stability. *Journal of the American Chemical Society*, **141**, 9207–9216.

Douplik A., Saiko G., Schelkanova I., Tuchin V.V. (2013) The response of tissue to laser light. In *Lasers for Medical Applications*, pp. 47–109: Elsevier.

Errington J., van der Aart L.T. (2020) Microbe Profile: Bacillus subtilis: model organism for cellular development, and industrial workhorse. *Microbiology*, **166**, 425.

Gilbert Y., Deghorain M., Wang L., Xu B., Pollheimer P.D., Gruber H.J., Errington J., Hallet B., Haulot X., Verbelen C. (2007) Single-molecule force spectroscopy and imaging of the vancomycin/D-Ala-D-Ala interaction. *Nano letters*, **7**, 796–801.

Hayhurst E.J., Kailas L., Hobbs J.K., Foster S.J. (2008) Cell wall peptidoglycan architecture in Bacillus subtilis. *Proceedings of the National Academy of Sciences*, **105**, 14603–14608.

Jahng J., Kim B., Lee E.S., Potma E.O. (2016) Quantitative analysis of sideband coupling in photoinduced force microscopy. *Physical Review B*, **94**, 195407.

Jahng J., Potma E.O., Lee E.S. (2018) Tip-enhanced thermal expansion force for nanoscale chemical imaging and spectroscopy in photoinduced force microscopy. *Analytical chemistry*, **90**, 11054–11061.

Ji B., Kenaan A., Gao S., Cheng J., Cui D., Yang H., Wang J., Song J. (2019) Label-free detection of biotoxins via a photo-induced force infrared spectrum at the single-molecular level. *Analyst*, **144**, 6108–6117.

Kahne D., Leimkuhler C., Lu W., Walsh C. (2005) Glycopeptide and lipoglycopeptide antibiotics. *Chemical reviews*, **105**, 425–448.

Katzenmeyer A.M., Holland G., Kjoller K., Centrone A. (2015) Absorption spectroscopy and imaging from the visible through mid-infrared with 20 nm resolution. *Analytical chemistry*, **87**, 3154–3159.

Le Wang, Jakob D.S., Wang H., Apostolos A., Pires M.M., Xu X.G. (2019) Generalized Heterodyne Configurations for Photoinduced Force Microscopy. *Analytical chemistry*, **91**, 13251–13259.

Li J., Jahng J., Pang J., Morrison W., Li J., Lee E.S., Xu J.-J., Chen H.-Y., Xia X.-H. (2020) Tip-Enhanced Infrared Imaging with Sub-10 nm Resolution and Hypersensitivity. *The Journal of Physical Chemistry Letters*, **11**, 1697–1701.

Li K., Yuan X.-X., Sun H.-M., Zhao L.-S., Tang R., Chen Z.-H., Qin Q.-L., Chen X.-L., Zhang Y.-Z., Su H.-N. (2018) Atomic force microscopy of side wall and septa peptidoglycan from Bacillus subtilis reveals an architectural remodeling during growth. *Frontiers in microbiology*, **9**, 620.

Lima C., Muhamadali H., Xu Y., Kansiz M., Goodacre R. (2021) Imaging Isotopically Labeled Bacteria at the Single-Cell Level Using High-Resolution Optical Infrared Photothermal Spectroscopy. *Analytical chemistry*.

Lottspeich F., Engels J.W. (2012) *Bioanalytik.* 3rd edn. Berlin Heidelberg: Springer.

Madigan M. (2005) Martinko J. Brock biology of microorganisms. *Int. Microbiol*, **8**.

Mayet C., Dazzi A., Prazeres R., Allot F., Glotin F., Ortega J.M. (2008) Sub-100 nm IR spectromicroscopy of living cells. *Optics letters*, **33**, 1611–1613.

McComas C.C., Crowley B.M., Boger D.L. (2003) Partitioning the loss in vancomycin binding affinity for D-Ala-D-Lac into lost H-bond and repulsive lone pair contributions. *Journal of the American Chemical Society*, **125**, 9314–9315.

McStrother (2011) Vancomycin action and resistance. URL https://commons.wikimedia.org/wiki/File:Vancomycin_resistance.svg.

MolecularVista (2021) Scientific Principles of PiFM and PiF-IR. URL https://molecularvista.com/technology/pifm-and-pif-ir/scientific-principles/.

Molinari H., Pastore A., Lian L.Y., Hawkes G.E., Sales K. (1990) Structure of vancomycin and a vancomycin/D-Ala-D-Ala complex in solution. *Biochemistry*, **29**, 2271–2277.

Müller G. (2013) *Grundlagen der Lebensmittelmikrobiologie: eine Einführung*: Springer-Verlag.

Naumann D., Labischinski H., Rönspeck W., Barnickel G., Bradaczek H. (1987) Vibrational spectroscopic analysis of LD-sequential, bacterial cell wall peptides: an IR and Raman study. *Biopolymers: Original Research on Biomolecules*, **26**, 795–817.

Nowak D., Morrison W., Wickramasinghe H.K., Jahng J., Potma E., Wan L., Ruiz R., Albrecht T.R., Schmidt K., Frommer J. (2016) Nanoscale chemical imaging by photoinduced force microscopy. *Science advances*, **2**, e1501571.

Olson N.E., Xiao Y., Lei Z., Ault A.P. (2020) Simultaneous Optical Photothermal Infrared (O-PTIR) and Raman Spectroscopy of Submicrometer Atmospheric Particles. *Analytical chemistry*, **92**, 9932–9939.

Otter L.M., Förster M.W., Belousova E., O'Reilly P., Nowak D., Park S., Clark S., Foley S.F., Jacob D.E. (2021) Nanoscale Chemical Imaging by Photo-Induced Force Microscopy: Technical Aspects and Application to the Geosciences. *Geostandards and Geoanalytical Research*, **45**, 5–27.

Padalkar M.V., Pleshko N. (2015) Wavelength-dependent penetration depth of near infrared radiation into cartilage. *Analyst*, **140**, 2093–2100.

Pereira P.M., Filipe S.R., Tomasz A., Pinho M.G. (2007) Fluorescence ratio imaging microscopy shows decreased access of vancomycin to cell wall synthetic sites in vancomycin-resistant Staphylococcus aureus. *Antimicrobial agents and chemotherapy*, **51**, 3627–3633.

Photothermal Spectroscopy Corporation (2020) *mIRage system manual*. 325 Chapala St., Santa Barbara, CA 93101.

Rao J., Colton I.J., Whitesides G.M. (1997) Using capillary electrophoresis to study the electrostatic interactions involved in the association of D-Ala-D-Ala with vancomycin. *Journal of the American Chemical Society*, **119**, 9336–9340.

Salzer R., Siesler Heinz W. (Eds) (2014) *Infrared and Raman Spectroscopic Imaging.* Second, Completely Revised, and Updated Edition. Weinheim: Wiley-VCH.

Spadea A., Denbigh J., Lawrence M.J., Kansiz M., Gardner P. (2021) Analysis of Fixed and Live Single Cells Using Optical Photothermal Infrared with Concomitant Raman Spectroscopy. *Analytical chemistry*.

Stein T. (2005) Bacillus subtilis antibiotics: structures, syntheses and specific functions. *Molecular microbiology*, **56**, 845–857.

Stein T. (2020) Oxygen-Limiting Growth Conditions and Deletion of the Transition State Regulator Protein Abrb in Bacillus subtilis 6633 Result in an Increase in Subtilosin Production and a Decrease in Subtilin Production. *Probiotics and antimicrobial proteins*, **12**, 725–731.

Stogios P.J., Savchenko A. (2020) Molecular mechanisms of vancomycin resistance. *Protein Science*, **29**, 654–669.

Tortora G.J., Funke B.R., Case C.L. (2007) *Microbiology: an introduction*: Pearson Benjamin Cummings San Francisco, CA.

Vollmer W., Bertsche U. (2008) Murein (peptidoglycan) structure, architecture and biosynthesis in Escherichia coli. *Biochimica et Biophysica Acta (BBA)-Biomembranes*, **1778**, 1714–1734.

Wang F., Zhou H., Olademehin O.P., Kim S.J., Tao P. (2018) Insights into key interactions between vancomycin and bacterial cell wall structures. *ACS omega*, **3**, 37–45.

Wheeler R., Mesnage S., Boneca I.G., Hobbs J.K., Foster S.J. (2011) Super-resolution microscopy reveals cell wall dynamics and peptidoglycan architecture in ovococcal bacteria. *Molecular microbiology*, **82**, 1096–1109.

Wickramasinghe H.K., Park S. (2015) Force detection of IR response at sub-10nm resolution. *SPIE Newsroom*, 1–3.

Xiao L., Schultz Z.D. (2018) Spectroscopic imaging at the nanoscale: technologies and recent applications. *Analytical chemistry*, **90**, 440–458.

# Attachment

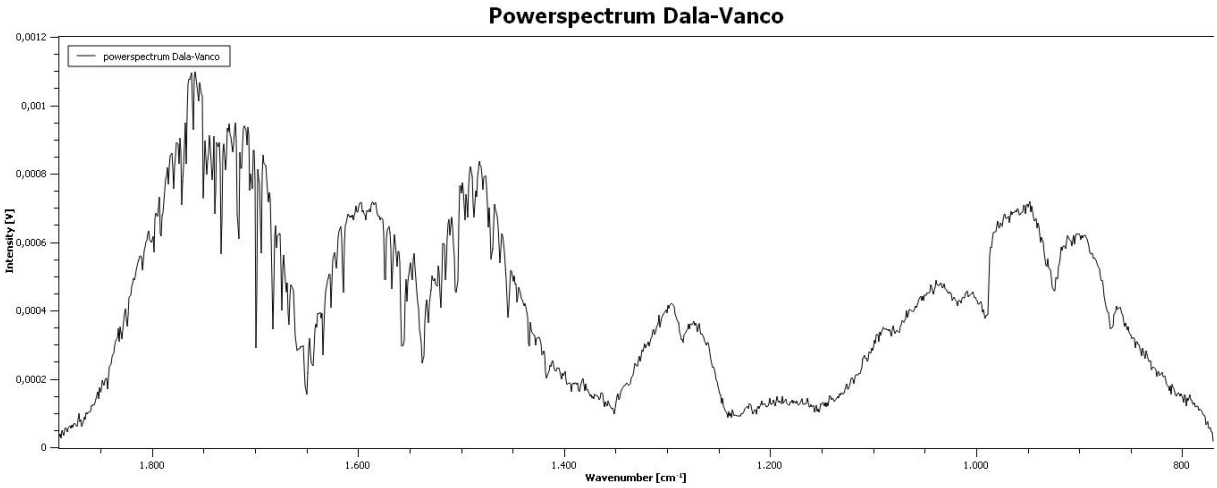


*Figure A 1: exemplary powerspectrum from PiFM acquired with 100% IR- laser intensity*

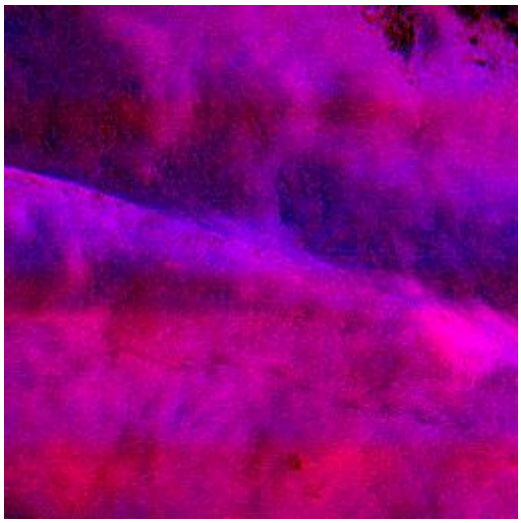

*Figure A 2: striped pattern (based on the running cooling of the instrument) within the RGB image of overlayed PiFM single wavenumber scans of untreated control at 30 minutes of the sugar and Vancomycin peak 1060 $cm^{-1}$ (blue) and the interaction-based wavenumber 1520 $cm^{-1}$ (red)*

# Declaration of independence

I hereby confirm that the submitted thesis is original work and was written by me without further assistance. Appropriate credit has been given where reference has been made to the work of others. The thesis was not examined before, nor has it been published. The submitted electronic version of the thesis matches the printed version.

# Eigenständigkeitserklärung

Hiermit versichere ich, dass ich die von mir vorgelegte Masterarbeit selbständig verfasst habe, keine anderen als die in der Masterarbeit angegebenen Quellen und Hilfsmittel benutzt habe und ich alle wörtlich oder sinngemäß aus anderen Werken übernommenen Inhalte als solche kenntlich gemacht habe. Des Weiteren versichere ich, dass die von mir vorgelegte Masterarbeit weder vollständig noch in wesentlichen Teilen Gegenstand eines anderen Prüfungsverfahrens war oder ist. Ich versichere zudem, dass die von mir eingereichte elektronische Version in Form und Inhalt der gedruckten Version der Masterarbeit entspricht.

..... .....

Ort, Datum Unterschrift

Place, date Signature